Nano Today (2011) 6, 401—418

available at www.sciencedirect.com

ScienceDirect

journal homepage: www.elsevier.com/locate/nanotoday

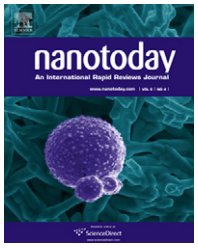

REVIEW

Ultra-small fluorescent metal nanoclusters: Synthesis and biological applications

Li Shang[a], Shaojun Dong[b], G. Ulrich Nienhaus[a,c,*]

[a] *Institute of Applied Physics and Center for Functional Nanostructures (CFN), Karlsruhe Institute of Technology (KIT), Wolfgang-Gaede-Strasse 1, 76131 Karlsruhe, Germany*
[b] *State Key Laboratory of Electroanalytical Chemistry, Changchun Institute of Applied Chemistry, Chinese Academy of Sciences, Changchun 130022, China*
[c] *Department of Physics, University of Illinois at Urbana-Champaign, Urbana, IL 61801, USA*

Received 24 March 2011; received in revised form 3 June 2011; accepted 19 June 2011
Available online 8 July 2011

KEYWORDS
Fluorescent probes;
Metal nanoclusters;
Bioanalysis;
Fluorescence imaging;
Biolabels

Abstract Recent advances in nanotechnology have given rise to a new class of fluorescent labels, fluorescent metal nanoclusters, e.g., Au and Ag. These nanoclusters are of significant interest because they provide the missing link between atomic and nanoparticle behavior in metals. Composed of a few to a hundred atoms, their sizes are comparable to the Fermi wavelength of electrons, resulting in molecule-like properties including discrete electronic states and size-dependent fluorescence. Fluorescent metal nanoclusters have an attractive set of features, such as ultrasmall size, good biocompatibility and excellent photostability, making them ideal fluorescent labels for biological applications. In this review, we summarize synthesis strategies of water-soluble fluorescent metal nanoclusters and their optical properties, highlight recent advances in their application for ultrasensitive biological detection and fluorescent biological imaging, and finally discuss current challenges for their potential biomedical applications.

Introduction

Nanobiotechnology, the integration of nanotechnology with biology, biochemistry and medicine, is an emerging and very active research field. Particularly, the utilization of nanostructured materials in biology and biomedicine has been extensively explored during the past decade [1,2]. The development of luminescent nanomaterials as fluorescent labels is an especially attractive research field due to the multitude of promising applications in the life sciences [3,4]. To date, researchers have developed several different types of luminescent nanomaterials, including semiconductor quantum dots (QDs) [5], dye-doped nanoparticles [6], up-converting lanthanide-doped nanoparticles [7] and carbon nanodots [8]. Compared with existing small-molecule dyes and fluorescent proteins [9], these luminescent nanoprobes exhibit much improved photophysical properties, huge surface-to-volume ratios, facile surface tailorability and color tunability. Consequently, they are

* Corresponding author at: Institute of Applied Physics and Center for Functional Nanostructures (CFN), Karlsruhe Institute of Technology (KIT), Wolfgang-Gaede-Strasse 1, 76131 Karlsruhe, Germany. Tel.: +49 721 608 43401; fax: +49 721 608 48480.
E-mail address: uli@uiuc.edu (G.U. Nienhaus).

1748-0132/$ — see front matter © 2011 Elsevier Ltd. All rights reserved.
doi:10.1016/j.nantod.2011.06.004

expected to complement or possibly even replace conventional fluorescent probes and offer great opportunities for advancing fields such as biosensors, molecular imaging, optoelectronics and nanomedicine.

Metal nanoclusters (NCs), composed of a few to roughly a hundred atoms, are a new type of luminescent nanomaterials that recently have attracted a great deal of interest [10—12]. Metal NCs typically have diameters below 2 nm and properties that place them between isolated atoms and larger nanoparticles or even bulk noble metals. For NC dimensions approaching the Fermi wavelength of electrons, the continuous density of states breaks up into discrete energy levels leading to the observation of dramatically different optical, electrical and chemical properties as compared to nanoparticles [10]. A distinct feature is their strong photoluminescence, combined with good photostability, large Stokes shift and high emission rates. Moreover, recent advances have enabled facile synthesis of water-soluble fluorescent metal NCs with different ligands and tunable emission colors in various biocompatible scaffolds, establishing them as a new class of ultrasmall, biocompatible fluorophores for applications as biological labels or optoelectronic emitters [13—15].

In this review, we will first summarize the synthesis strategies developed for these fluorescent metal NCs and describe their optical properties. While there are also a few reports on fluorescent metal NCs such as Cu [16] and Pt [17], this review focuses mainly on Au and Ag NCs. We highlight recent advances in the application of fluorescent metal NCs to the detection of various analytes including metal ions, small biomolecules, proteins and nucleic acids, as well as in biological imaging. In the final section, we discuss some of the challenges that researchers currently face in their research on fluorescent metal NCs.

Synthesis of fluorescent metal nanoclusters

Actually, the observation of photoluminescence from noble metals dates back more than forty years but has not attracted much attention due to the extremely low quantum yield (QY) of 10^{-10} [18]. Recently, however, researchers have developed various approaches to synthesize water-soluble fluorescent metal NCs with much enhanced QY in the range of 10^{-3} to 10^{-1}, thus sufficiently bright for fluorescence marker applications. In general, the reduction of metal ions in aqueous solution results in large nanoparticles rather than small NCs due to the tendency of NCs to aggregate. In addition, the nature of the ligands used for capping the particle surface can markedly affect their emission properties [19]. Therefore, choosing suitable agents capable of stabilizing clusters from aggregating and enhancing their fluorescence is of key importance for obtaining small, highly fluorescent metal NCs. Accordingly, we will discuss the various synthesis strategies of fluorescent metal NCs based on different types of stabilizers.

Thiols

Thiol-containing small molecules are the most commonly adopted stabilizers in metal nanoparticle synthesis owing to the strong interaction between thiols and Au/Ag [20]. Glutathione was shown to be an excellent stabilizer for synthesizing Au NCs with visible luminescence by reducing Au^{3+} in the presence of glutathione with sodium borohydride ($NaBH_4$); the QY of these NCs was reported to be in the order of 10^{-3} [21]. A series of glutathione-protected Au NCs with defined chemical compositions have been synthesized [22,23]. In similar approaches, fluorescent Au NCs stabilized with various other thiols such as tiopronin [24], phenylethylthiolate [25], thiolate α-cyclodextrin [26] and 3-mercaptopropionic acid [27] have also been reported. Using bidentate dihydrolipoic acid (DHLA) as the stabilizing agent, Adhikari and Banerjee [28] recently reported the synthesis of fluorescent Ag NCs (QY: 2%) by reducing a mixture of lipoic acid and Ag^+ with $NaBH_4$. Note that the particle size as well as the luminescence efficiency of metal NCs prepared by this approach depends sensitively on the thiol-to-metal molar ratio. Increasing this ratio will result in smaller metal NCs and, correspondingly, in a blue-shift of the emission wavelength. While thiol-stabilized metal NCs were mostly produced by using the strong reductant $NaBH_4$, the Nienhaus group [29] recently reported Au NC synthesis by using a mild reductant, tetrakis(hydroxymethyl)phosphonium chloride (THPC). In this approach, a zwitterionic thiolate ligand, D-penicillamine (DPA), was chosen as the stabilizer (Fig. 1). The obtained DPA-capped Au NCs emitted bright fluorescence at 610 nm (QY: 1.3%) and possessed excellent stability in aqueous solvents over the physiologically relevant pH range.

In addition to the above-mentioned one-pot strategy by direct reduction of metal ions in the presence of thiols, luminescent, monolayer-protected metal NCs can also be

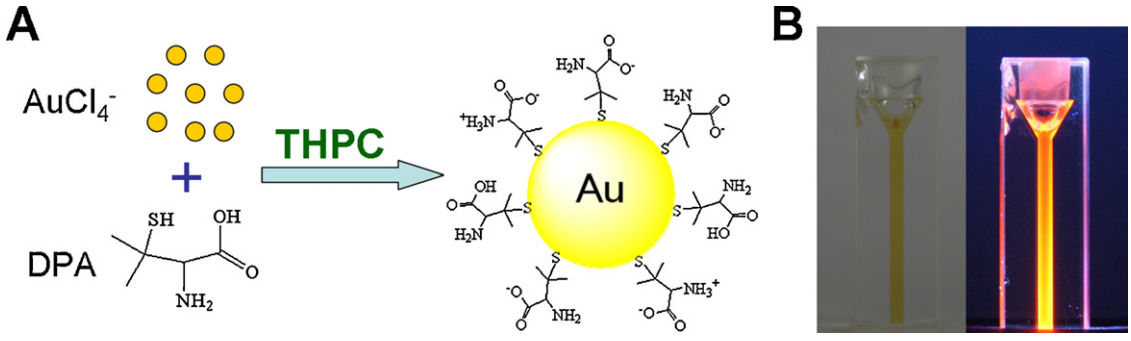

Fig. 1 (A) Schematic depiction of the synthesis of DPA-stabilized fluorescent Au NCs using THPC as the reductant. (B) Photographs of an aqueous solution of DPA-Au NCs (left) in room light and (right) under a UV light source with excitation at 365 nm.

produced by etching large Au nanoparticles with thiols. Chang and coworkers [30] produced fluorescent Au NCs by adding various alkanethiol ligands to preformed Au nanoparticles stabilized by THPC. TEM measurement revealed that the size of the particles decreased with increasing size of the thiol-capping agent. 11-mercaptoundecanoic acid (11-MUA) was found to yield the brightest Au NCs, with a QY of 3.1%. By controlling the molar ratios of THPC to Au/Ag ions, they further showed that fluorescent Au and Au/Ag NCs with tunable size and emission wavelength could be obtained by using this strategy with 11-MUA as capping agent [31]. Along a similar route, Chang and coworkers [32] also prepared α-D-mannose-conjugated Au NCs through the reaction of Au nanoparticles with thiol-modified mannose. Interestingly, irradiation with a light-emitting diode (LED) during preparation was shown to enhance the QY, alter the emission wavelength and shorten the reaction time. Under illumination by a green LED, luminescent, mannose-conjugated Au NCs with QY of 11% were prepared within 8 h.

Fluorescent Au NCs by etching nanoparticles were also prepared using other capping agents. Pradeep et al. [33] synthesized fluorescent Au NCs from mercaptosuccinic acid (MSA)-protected Au nanoparticles by etching with excess glutathione. The etching process was found to be pH-dependent: etching at pH 3 and 7–8 yielded Au_{25} and Au_8, respectively. Two possible mechanisms were proposed to explain this etching-based strategy (Fig. 2). Along the first route, gold atoms are removed from the nanoparticle surfaces by excess ligands (such as glutathione) in the form of Au(I)-thiolate complexes, which then undergo strong aurophilic interactions and form luminescent Au clusters. Alternatively, ligands may etch the surface gold atoms of the nanoparticles, leading to the formation of luminescent particles with decreased size, and the removed atoms will precipitate as Au(I)-thiolate complexes after etching. The same group also developed an interfacial route for the synthesis of brightly red-emitting Au_{23} clusters by core etching of more stable, glutathione-protected Au_{25} clusters [34]. In recent work, fluorescent Au NCs were synthesized based on precursor-induced etching in the organic phase from didodecyldimethylammonium bromide (DDAB)-stabilized Au nanoparticles [35]. The clusters became highly red-luminescent upon ligand exchange with DHLA for the transfer of the product to aqueous solution (QY: 3.45%).

The etching-based strategy has also been used to synthesize thiol-protected fluorescent Ag NCs. Ag NCs were produced through interfacial etching of MSA-protected Ag nanoparticles with excess MSA at the water–organic interface [36]. A crude mixture of luminescent Ag_7 and Ag_8 clusters was finally obtained by this approach. Unfortunately, the approaches developed for the synthesis of Au NCs are not always successful for the synthesis of their Ag analogues. Therefore, researchers aim to develop other facile routes to prepare monolayer-protected Ag NCs. Recently, a new solid-state route was introduced to prepare luminescent Ag_9 NCs protected with MSA (QY: 0.8%) [37]. Remarkably, these Ag NCs can be synthesized in gram quantities by minimizing diffusion of the reactants in the growth step by mixing them in the solid state. This new synthetic approach is expected to be applicable to the synthesis of other metal clusters as well.

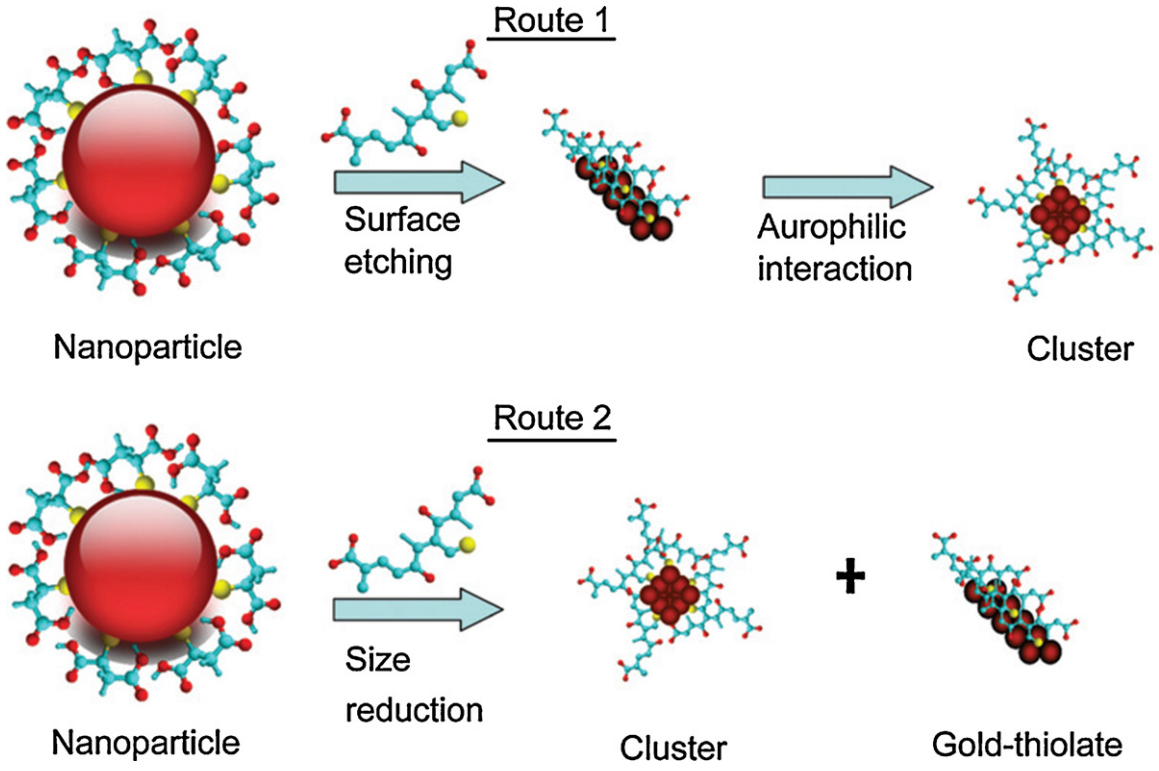

Fig. 2 Schematic illustration of two possible routes for the formation of luminescent Au NCs via etching of preformed MSA-protected Au nanoparticles.
(Reprinted with permission from Reference [33] ©2008 Springer.)

Dendrimers

Based on their capability of sequestering metal ions from solution, dendrimers have been utilized as templates to prepare small metal NCs. In a remarkable paper, Dickson and colleagues [38] reported the first synthesis of photostable luminescent Ag NCs in PAMAM dendrimers through direct photoreduction. Subsequently, they described the synthesis of fluorescent, dendrimer-stabilized Au_8 NCs with a high QY of 42% [39]. Moreover, Au NCs with emission colors ranging from the UV to the near-infrared (NIR) region were obtained by varying the relative PAMAM/Au concentration and the dendrimer generation [40]. This approach, however, has the disadvantage of low synthesis yield of small NCs owing to the simultaneous formation of large nanoparticles. Martinez et al. [41] subsequently developed a new approach for synthesizing fluorescent PAMAM-templated Au NCs that avoids the formation of large nanoparticles. They produced small fluorescent Au NCs at physiological temperature using a mild biologically derived reductant, ascorbic acid. Recently, Lin et al. [42] proposed a simple strategy for synthesizing dendrimer-encapsulated Au NCs (predominantly Au_8). By introducing a specific counterion (AuX_4^-, X = chloride or bromide) into a dendritic microcavity with pH-dependent polarity, dendrimer-encapsulated Au NCs with high QY (20—62%) were obtained upon microwave irradiation.

Polymers

Polymers with abundant carboxylic acid groups were identified as promising templates for synthesizing highly fluorescent, water-soluble Ag NCs. In an earlier report, fluorescent Ag NCs were prepared in polymer microgels of poly(N-isopropylacrylamide-acrylic acid-2-hydroxyethyl acrylate) by UV irradiating the mixture of polymer microgel and Ag^+ [43]. Similarly, a molecular hydrogel composed of multi-arm star polyglycerol-block-poly(acrylic acid) copolymers was used for synthesizing fluorescent Ag NCs via photoreduction by Frey and coworkers [44]. With a commercially available polyelectrolyte, poly(methacrylic acid) (PMAA), as a template, Shang and Dong [45] presented a simpler and cheaper approach to prepare water-soluble fluorescent Ag NCs under photoreduction. Upon UV irradiation (365 nm) of a silver salt aqueous solution in the presence of PMAA, highly fluorescent Ag NCs were obtained with a QY of 18.6%. Ras et al. [46] further showed that such PMAA-Ag NCs, prepared by photoactivation using visible light, exhibited electrochemiluminescent and solvatochromic properties. While photoreduction has proved useful for synthesizing Ag NCs, fluorescent PMAA-Ag NCs have also been produced via convenient sonochemical [47] and microwave-assisted approaches [48].

There are also several recent reports on the synthesis of polymer-stabilized fluorescent Au NCs. For instance, Au NCs capped with multivalent polymers, polyethylenimine (PEI), were prepared by etching preformed dodecylamine-capped Au nanoparticles [49]. These fluorescent clusters exhibited strong blue emission with a QY of 10—20%. Cooper et al. [50] reported the synthesis of fluorescent multidentate, polymer-capped Au NCs by $NaBH_4$ reduction. Their polymer consisted of a linear chain of water-soluble methacrylic acid units and a hydrophobic end group containing three unreacted thiols. Upon systematic variation of the polymer-to-gold ratio, a transition from non-fluorescent to fluorescent nanoparticles was observed for particle diameters between 1.1 nm and 1.7 nm. Au NCs consisting of only two or three atoms protected by poly(N-vinylpyrrolidone) (PVP) have been synthesized via a simple electrochemical technique by Santiago González et al. [51]. These PVP-Au NCs showed not only stable photoluminescence but also magnetic properties (Fig. 3). Compared with previous methods of producing small metal NCs, the electrochemical synthesis is much simpler and quicker, providing a good

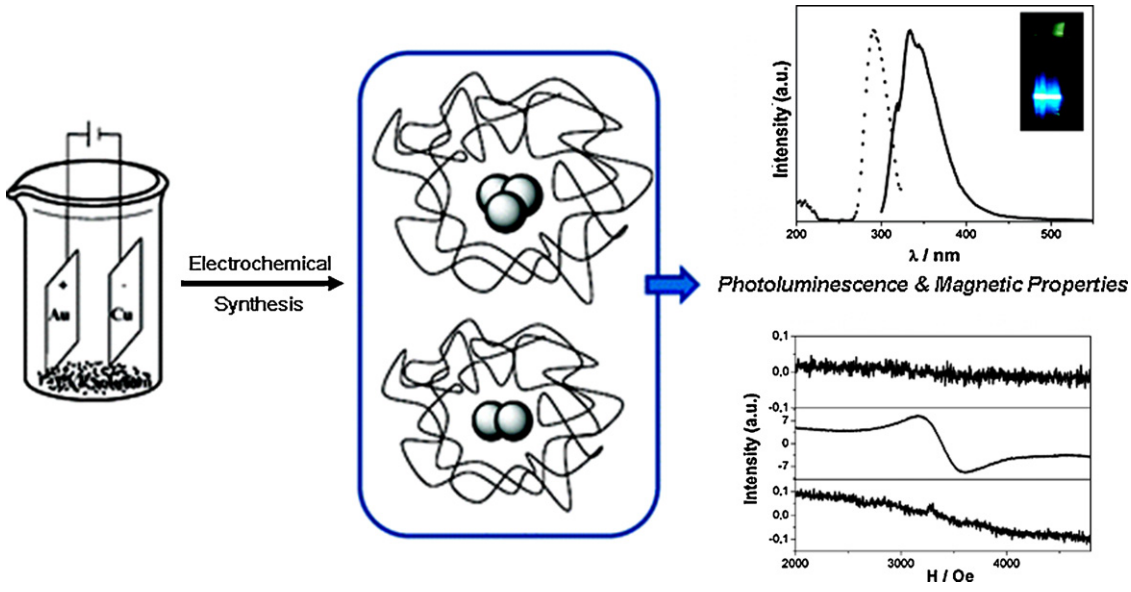

Fig. 3 Synthesis of Au NCs containing only two and three atoms in the presence of PVP via simple electrochemical technique. These clusters show stable photoluminescent and magnetic properties.
(Reprinted with permission from Reference [51] ©2010 American Chemical Society.)

control over the cluster size. Most recently, Yabu [52] synthesized blue-emitting Au NCs via reflux of Au ions with amino-terminated poly(1,2-butadiene) (PB-NH_2) in toluene. Photoluminescent composite films of PB-NH_2 and Au NCs were patterned through photo-crosslinking of PB.

DNA oligonucleotides

The well known interactions of metal cations with DNA have enabled the design and fabrication of various DNA-templated metal nanostructures [53]. Especially silver ions possess a high affinity to cytosine bases on single-stranded DNA, which makes DNA oligonucleotides good stabilizers for preparing small Ag NCs [54,55]. In a pioneering study, Dickson and coworkers [56] reported the synthesis of short oligonucleotide-encapsulated Ag NCs by using $NaBH_4$ as the reductant. Mass spectroscopy demonstrated the formation of small Ag NCs with 1—4 atoms bound to the 12-base oligonucleotide, and distinct absorption and fluorescence spectral features were observed. NMR spectroscopy further revealed that cytosine experienced the largest chemical shifts with Ag NCs. Based on these findings, red- and blue/green-emitting Ag NCs were then prepared with 12-mer cytosine as template [57,58]. Several studies were carried out that emphasize the key role of bases and base sequences on the formation of oligonucleotide-stabilized fluorescent Ag NCs [59—62]. For instance, Petty et al. [59] found that the bases have a dominant influence on cluster formation, and both base complexation and inherent cluster stability contribute to the type of DNA-encapsulated Ag NCs. Gwinn et al. [60] demonstrated that both sequence and secondary structure of the oligonucleotide strand can affect the fluorescence properties of these DNA-hosted Ag NCs.

Using DNA microarrays for high-throughput analysis of 12-mer oligonucleotide strands to identify optimal sequences for Ag NC formation, well-defined fluorescent Ag NCs with distinct emission ranging from blue to NIR were produced, although the synthesis of each specific NCs did not follow a general procedure (Fig. 4) [63]. These Ag NCs were reported to possess high QYs in the range of 16—34%. Particularly, the yellow, red and NIR emitting species showed greatly reduced bleaching and blinking, suggesting significant advantages over existing dyes for single molecule spectroscopy and imaging. O'Neill et al. [64] presented the loop-dependent synthesis of fluorescent Ag NCs on DNA hairpins with 3—12 cytosines in the loop. Their results showed that the number of cytosines in the loop could tune the stability and fluorescence of Ag NCs. Moreover, mismatched double-stranded DNA templates have recently been utilized for the site-specific growth of fluorescent Ag NCs [65]. Molecular-scale Ag NCs were found to localize in the mismatched site while the metalized DNA retains its integrity.

Contrary to many studies on DNA-encapsulated Ag NCs, studies on the synthesis of luminescent Au NCs with DNA as the capping agent are scarce, with the exception of a recent study by Chen et al. [66]. They showed that atomically monodisperse Au NCs could be obtained by etching gold particles (either spheres or rods) with the assistance of biomolecules including amino acids, proteins and DNA under sonication in water. Specifically, Au nanorods were gradually

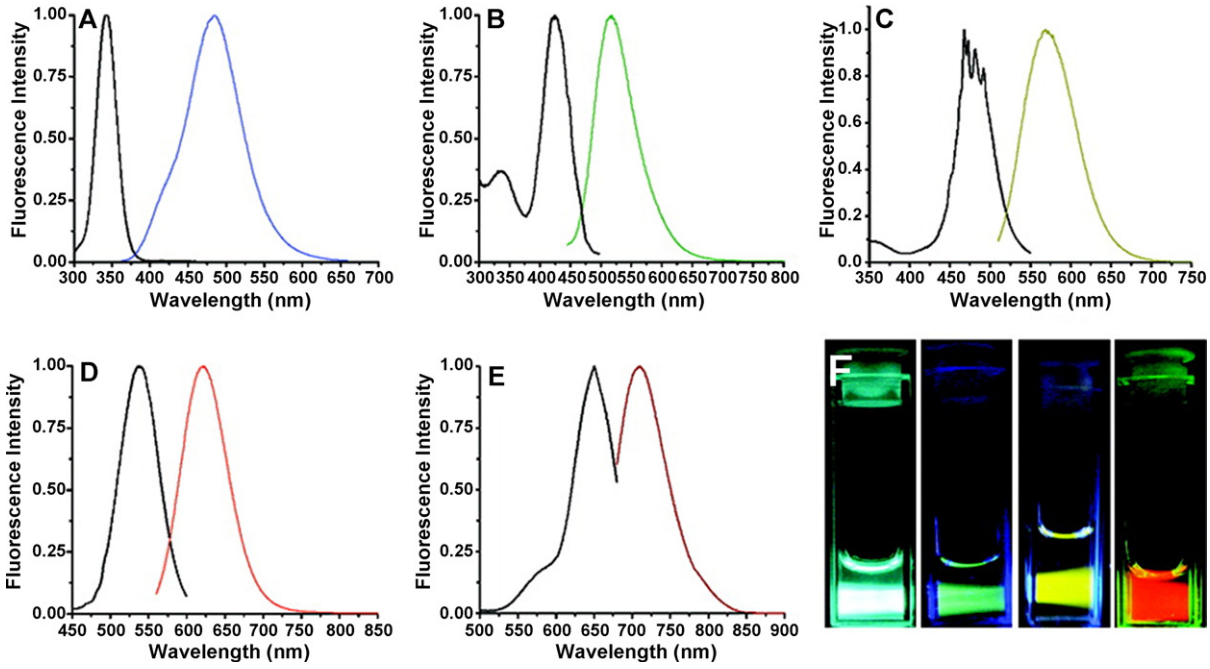

Fig. 4 Steady-state excitation and emission spectra for five distinct ss-DNA encapsulated Ag NCs. (A) Blue emitters created in 5′-CCCTTTAACCCC-3′, (B) green emitters created in 5′-CCCTCTTAACCC-3′, (C) yellow emitters created in 5′-CCCTTAATCCCC-3′, (D) red emitters created in 5′-CCTCCTTCCTCC-3′, and (E) near-IR emitters created in 5′-CCCTAACTCCCC-3′. (F) Images of dissolved NCs, the spectra of which are shown in panels A—D (from left to right).
(Reprinted with permission from Reference [63] ©2008 American Chemical Society.)

etched by double-stranded DNA under sonication, leading to the formation of fluorescent Au_8 NCs. The involvement of violent sonication during synthesis, however, may lead to the disruption of the DNA structures.

Peptides and proteins

Biological macromolecules such as peptides and proteins have also been utilized as templates for synthesizing highly fluorescent metal NCs. Dickson and coworkers [67] reported a significant advance in producing fluorescent Ag NCs in vivo by ambient-temperature photoactivation. A protein, nucleolin, which is known to bind silver, was employed as the major scaffold for the formation of fluorescent Ag NCs. Inspired by this observation, they further designed a short peptide incorporating the specific amino acids most prevalent in nucleolin and several cysteine groups to form and stabilize fluorescent Ag NCs directly in phosphate buffered solution. A short peptide-based hydrogel was also used to produce fluorescent Ag NCs by Adhikari and Banerjee [68]. Interestingly, Ag NCs containing only Ag_2 formed simply in the presence of sunlight at physiological pH. Apparently, Ag^+ ions associate with the carboxylate group of the aspartic acid residue in the gelator peptide and are spontaneously reduced under sunlight.

Compared with short peptides, large and complicated proteins possess abundant binding sites that can potentially bind and further reduce metal ions, thus offering better scaffolds for template-driven formation of small metal NCs. The first fluorescent Au NCs synthesized with proteins as templates were reported by Ying and coworkers in 2009 [69]. Based on the capability of bovine serum albumin (BSA) to sequester and reduce Au precursors in situ, they developed a simple, green synthetic route for the preparation of Au NCs with red emission (Fig. 5, QY: 6%). Notably, BSA functions both as a stabilizing agent and a reductant in this approach. As a matter of fact, the process is similar to the biomineralization behavior of organisms in nature. This work is remarkable not only for providing an alternative approach of synthesizing highly fluorescent Au NCs, but also because the proposed strategy may be extended to other proteins and metals. Inspired by this finding, researchers recently reported that other proteins such as lysozyme [70] and transferrin [71,72] could also act as efficient bioscaffolds for producing fluorescent Au NCs. Even denatured BSA has been shown to function as an effective stabilizing agent for fluorescent Ag NCs when using $NaBH_4$ as a reductant for cluster formation [73]. Besides their known roles as reductants and capping agents, proteins such as BSA can also function as etching agents for the synthesis of fluorescent Au NCs, according to a recent report by the Pradeep group [74].

Enzymes are proteins capable of catalyzing specific chemical reactions. The production of metal NCs directed by enzymatic activity can integrate the catalysis function of enzymes and the luminescence of metal NCs in a single cluster, thus leading to the possibility of constructing multi-functional nanoprobes. In a recent study, horseradish peroxidase (HRP) was used for templating the synthesis of fluorescent Au NCs under physiological conditions to form HRP—Au NC bioconjugates [75]. The fluorescence of HRP—Au NCs could be quenched quantitatively by adding H_2O_2, indicating that the HRP enzyme remains active in the luminescent conjugates. This study could be extended to other functional proteins to generate bifunctional Au NCs. Prior to this work, Narayanan and Pal [76] also reported a synthesis of luminescent Ag NCs templated by an enzyme, bovine pancreatic α-chymotrypsin, via $NaBH_4$ reduction. The functional integrity of the enzyme conjugated to Ag NCs was confirmed by monitoring the enzyme activity by absorption spectroscopy. The large excess of $NaBH_4$, however, caused adverse effects in the system, possibly affecting potential bioapplications.

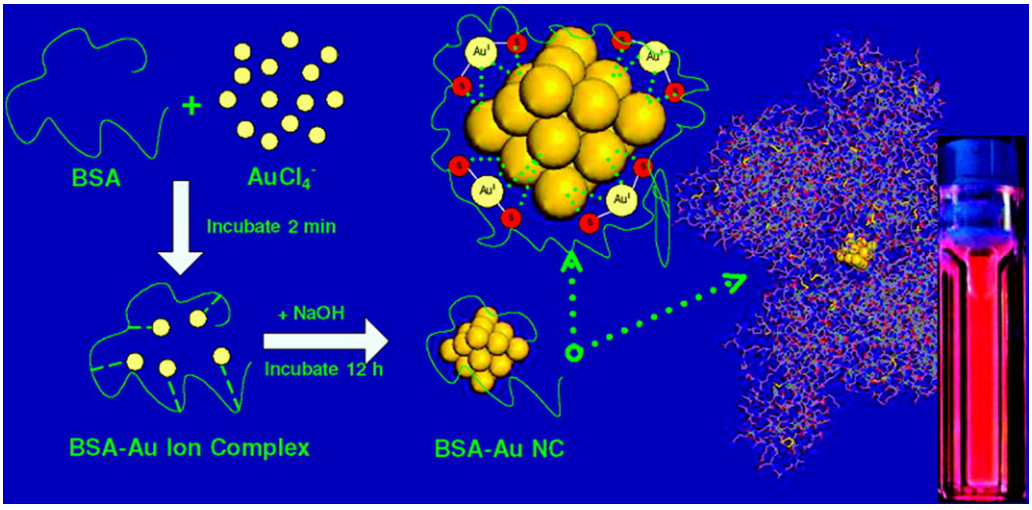

Fig. 5 Schematic representation of the formation of Au NCs in BSA solution. Upon adding Au(III) ions to the aqueous BSA solution, the protein molecules sequestered Au ions and entrapped them. The reducing capability of BSA was subsequently activated by adjusting the pH to about 12 with NaOH, so the entrapped ions underwent progressive reduction to form Au NCs in situ.
(Reprinted with permission from Ref. [69] ©2009 American Chemical Society.)

Optical properties of fluorescent metal nanoclusters

Absorption and fluorescence

Generally, the optical properties of metal nanoparticles are dominated by the collective oscillation of electrons at their surfaces, known as surface plasmon resonance, that are in resonance with the incident electromagnetic radiation. As the size reduces to the subnanometer scale, metal clusters are too small to support plasmons, and a transition from metal to molecule ensues. Instead of forming continuous densities of states and behaving as conductors, these few-atom metal NCs exhibit discrete energy levels. Well-defined metal NCs are expected to possess characteristic absorption features and can be distinguished from each other by their absorption profiles [34]. For instance, glutathione-protected Au_{25} NCs exhibit several characteristic absorption features in the range 400—1000 nm, which are believed to arise from intraband (sp ← sp) or interband transitions (sp ← d) of the bulk gold [77]. Tsukuda et al. [22] further showed that the absorption peaks of glutathione-protected Au NCs due to intraband transition tend to be blue-shifted with decreasing core size. As the size decreases, the spacing between the discrete states in each band increases, thus leading to a blue shift in the absorption peaks with decreasing cluster size. Absorption spectra of a few-atom Ag NCs also exhibit discrete electronic transitions instead of collective plasmon excitations. For example, Dickson and coworkers [56] reported fluorescent Ag_1—Ag_4 clusters with absorption peaks at 440 nm and 357 nm. In recent work, DHLA-protected Ag_4 and Ag_5 NCs were found to exhibit peaks at 435 nm and 335 nm, respectively, with another shoulder peak at 500 nm [28]. Discrete electronic transitions clearly indicate that these few atom metal NCs exhibit molecular behavior.

Luminescence of metals is normally extremely weak, owing to the efficient nonradiative decay and the absence of an energy gap [18]. However, recent studies showed that small metal NCs behave as ''artificial atoms'' and show photoluminescence with much enhanced QY, which can be seven to nine orders of magnitude higher than that of bulk gold (10^{-10}). With the rapid development of synthesis strategies, the luminescence properties of metal NCs have fascinated the scientific community. Compared with conventional fluorophores such as organic dyes and fluorescent proteins [78—80], metal NCs show advantageous photophysical properties including good photostability, large Stokes shift (over 100 nm) and high emission rate.

Currently, several mechanisms have been proposed to explain the emission properties of ultrasmall metal NCs. Huang and Murray [24,81] suggested that the visible luminescence of monolayer-protected metal NCs is associated with interband transitions between the filled d band and the sp conduction band. Whetten et al. [21] attributed the infrared luminescence from glutathione-protected Au_{25} clusters to the relaxed radiative recombination across the HOMO—LUMO gap within the sp conduction band (intraband transition). Chang et al. [32] suggested that the luminescence of their Au NCs, prepared via thiol-induced etching, mainly originated from Au NCs/polynuclear Au(I)-thiol (core/shell) complexes, based on the fact that these Au NCs displayed a strongly Stokes-shifted luminescence with long lifetimes (>100 ns), which is characteristic of thiol-Au(I) complexes that display ligand—metal charge transfer and metal—metal interactions. Zheng et al. [82] recently proposed that luminescent nanoparticles synthesized by dissociation of polymeric Au(I) thiolates can actually be considered as intermediate between luminescent Au(I) complexes/clusters and nonluminescent gold nanoparticles. More recently, Wu and Jin [19] reported that the surface ligands play a major role in the fluorescence of thiol-protected Au NCs. These studies suggest that there may be two major sources for the fluorescence of metal NCs: (1) the metal core, with its intrinsic quantization effects and (2) the particle surface, the properties of which are governed by the chemical interactions between the metal core and the surface ligands. Unlike QDs, no general mechanism is currently known that explains the emission from all metal NCs. Rather, the luminescence mechanism may be different for metal NCs with different sizes, coating ligands or even when they are prepared by different synthesis routes.

Solvatochromic effect

The solvatochromic effect is well known for larger metal nanoparticles and is mainly related to their surface plasmon phenomenon [83]. Several recent studies showed that few-atom metal NCs also display a similar dependence of their optical behavior on the solvent. Ras et al. [46] observed that both optical absorption and fluorescence emission properties of PMAA-stabilized Ag NCs could be tuned to a great extent by selecting appropriate solvents (Fig. 6). For instance, an about 70-nm red shift of the absorption peak of Ag NCs was observed upon transfer from water to methanol. Various DNA oligonucleotide-encapsulated Ag NCs were also found to exhibit strong, discrete fluorescence with solvent polarity-dependent absorption and emission [84]. Chen et al. [66] recently observed solvent-dependent photoluminescence properties of Au_8 NCs when exposed to different organic solvents such as chloroform, tetrahydrofuran, or N,N-dimethylformamide. In addition, they investigated the solvatochromic effect of Au_8 NCs protected by different ligands including histidine, cysteine and glutathione. The results were found to be independent of the type of coating on the cluster surface. The authors attributed the solvatochromic effect of Au NCs to the rich surface properties of the clusters. The change in chemical environment may induce electronic energy splitting and electron redistribution on the cluster surface, leading to a variation of the optical properties of the metal NCs [66]. While environment-sensitive optical properties of plasmonic metal nanoparticles have enabled the development of new techniques for sensitive chemical and biological sensing [85], we expect that the solvatochromic effect of fluorescent metal NCs may also be utilized in similar applications in the future.

Two-photon absorption

Compared with one-photon excitation, using two NIR photons of half the transition energy for the excitation of fluorophores can offer substantial advantages. In particular, for in vivo imaging and photodynamic therapy, two-photon

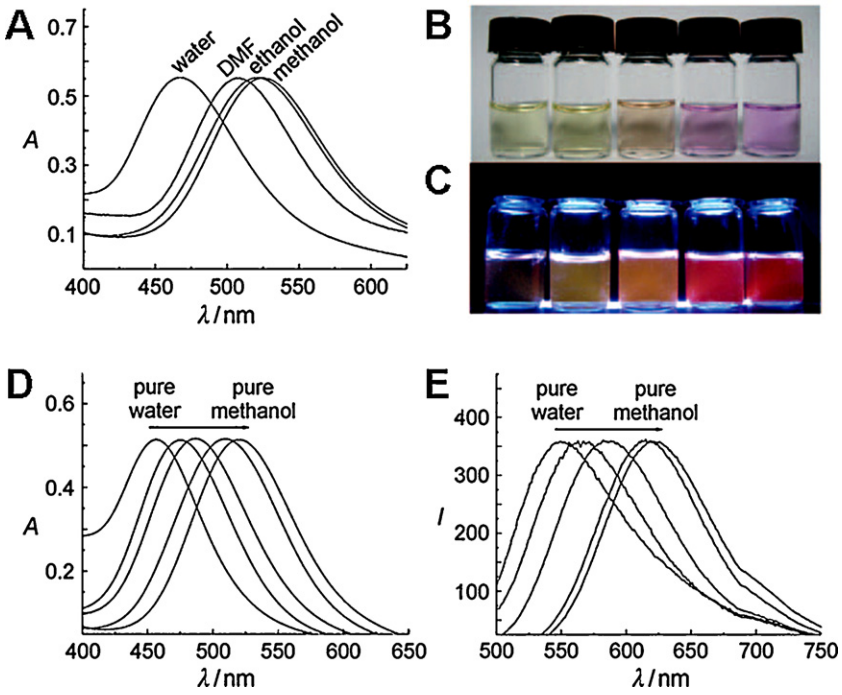

Fig. 6 Solvatochromic effects of PMAA-Ag NCs. (A) Absorption spectra in various solvents. Photograph of the NCs in water/methanol mixtures under (B) visible and (C) UV light, ranging from pure water (left) to pure methanol (right). (D) Absorption and (E) emission spectra of the samples shown in panel B.
(Reprinted with permission from Ref. [46] ©2009 Wiley—VCH.)

excitation (TPE) in the NIR region increases the penetration depth, spatial resolution due to lower scattering, and minimizes autofluorescence [86]. Goodson and coworkers [87] investigated two-photon absorption (TPA) properties of quantum sized Au_{25} NCs in hexane. Two-photon excited fluorescence in the visible region with excitation at 800 nm has been observed from these clusters, and the TPA cross-section was measured to be 42,700 GM (Göppert-Mayer unit, 10^{-50} cm^4 s), which is superior to the TPA cross-sections of many organic chromophores. The TPA properties of water-soluble 11-MUA-protected Au nanodots were studied by Chou et al. [88], who reported a TPA cross-section of about 8761 GM in water. Recently, strong two-photon emission from water-soluble glutathione-protected Au NCs was also observed [89]. The TPA cross-section of these Au NCs in water was determined to be 189,740 GM, much higher than those of typical organic dyes and QDs [90]. DNA-encapsulated Ag NCs were found to possess extremely high TPA cross-sections by Dickson et al. [91]. They quoted cross-sections of 35,000 GM for 660 nm Ag NCs, 34,000 GM for 680 nm emitters, and 50,000 GM for the 710 nm emitters. Such large TPA cross-sections of metal NCs make them efficient absorbers for multiphoton biological imaging and other nonlinear optical applications.

Electrochemiluminescence

Electrochemiluminescence (ECL) refers to the emission of light due to a high-energy electron transfer reaction between electrogenerated species, which possesses several advantages over photoluminescence in analytical chemistry, such as low cost and high sensitivity [92]. Ras et al. [46] first reported that PMAA-stabilized Ag NCs exhibited cathodic hot electron-induced ECL. They ascribed the ECL behavior of Ag NCs to the ox-red excitation pathway, where the luminophore was oxidized by the cathodically produced oxidizing radical, $SO_4^{\bullet -}$. However, the use of a voltage pulse of −30 V to obtain ECL of Ag NCs is unfavorable for real applications because unpredictable reactions can occur and, moreover, the surface structure of the electrode could be disrupted during the strong cathodic polarization [93]. Recently, Chen and coworkers [94] reported ECL from BSA-stabilized Au NCs using triethylamine as the co-reactant. A strong ECL signal was observed at ~1.45 V from Au NCs immobilized on the Pt electrode surface. Interestingly, the ECL spectrum in the presence of Au NCs showed a peak at 680 nm, located near the shoulder peak of Au NCs at 690 nm in the fluorescence emission spectrum, thus suggesting that the ECL mechanism may be related to the surface state of Au NCs. ECL from BSA-stabilized Au NCs on a modified indium tin oxide (ITO) electrode surface was observed by Zhu et al. [95], where $K_2S_2O_8$ was used as the co-reactant. In the cathodic ECL process, electrons were injected into the conduction band of ITO and then transferred to the LUMO of the Au NCs. A possible ECL mechanism was proposed as depicted in Fig. 7. A simple label-free method for dopamine detection was developed based on ECL of Au NCs in aqueous media, suggesting that water-soluble, biocompatible fluorescent metal NCs can be effective in the development of new types of ECL biosensors [95].

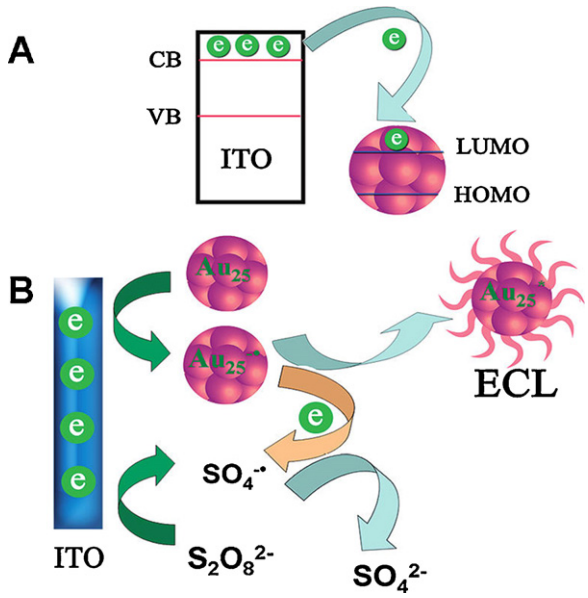

Fig. 7 Schematic illustration of (A) electron transfer between ITO and Au NCs and (B) the proposed ECL mechanisms of BSA-Au NCs.
(Reprinted with permission from Ref. [95] ©2011 American Chemical Society.)

Application of fluorescent metal nanoclusters in biodetection

Fluorescent metal NCs show great promise as optical reporters for sensitive biological detection, owing to their good water-solubility, large Stokes shifts, low toxicity and high emission rates. We summarize recent advances in the application of these emissive clusters for the detection of various biologically important analytes in this section.

Detection of metal ions

Hg^{2+} is a highly toxic and widespread pollutant ion, and its damaging effects to the brain, nervous system and the kidney even at very low concentrations are well known [96]. Recently, metal NCs have been utilized as Hg^{2+} sensors based on the quenching of their fluorescence. Chang et al. [30] showed that 11-MUA-capped Au NCs are capable of sensing Hg^{2+} based on Hg^{2+}-induced aggregation of Au NCs. The limit of detection (LOD) was measured to be 5.0 nM and a remarkable selectivity toward Hg^{2+} could be obtained when conducting the assay in the presence of a chelating ligand, 2,6-pyridinedicarboxylic acid (PDCA). BSA-stabilized Au NCs were demonstrated to be selective and sensitive for the detection of Hg^{2+} by Ying et al. [97]. The sensing mechanism was based on the high-affinity metallophilic Hg^{2+}—Au^{+} interactions, which efficiently quenched the fluorescence of Au NCs (Fig. 8). By virtue of the high QY of BSA-Au NCs, the LOD for Hg^{2+} was estimated to be 0.5 nM, which is much lower than the maximum level of mercury in drinking water (10 nM) permitted by the U.S. Environmental Protection Agency (EPA). Moreover, Lin and Tseng [98] showed that lysozyme type VI-stabilized Au NCs were capable of sensing Hg^{2+} and CH_3Hg^{+} through the interaction between Hg^{2+}/CH_3Hg^{+} and Au^{+} on the cluster surface. The LOD for Hg^{2+} and CH_3Hg^{+} were as low as 3 pM and 4 nM, respectively. This probe was successfully applied to the determination of both ions in seawater. Fluorescent oligonucleotide- and DHLA-stabilized Ag NCs have also been demonstrated recently for the determination of Hg^{2+} [28,99].

Cu^{2+} is another significant environmental pollutant and an essential trace element in biological systems. Considerable efforts have recently been directed at the detection of Cu^{2+} using fluorescent metal NCs. Shang and Dong [100] have developed a simple and sensitive fluorescent sensor for Cu^{2+} detection based on fluorescent PMAA-Ag NCs. The LOD of Cu^{2+} was measured to be 8 nM at a signal-to-noise (S/N) ratio of 3, which is much lower than the U.S. EPA limit for Cu^{2+} in drinking water (20 μM). The detection mechanism was based on the fluorescence quenching by Cu^{2+} upon interaction with the free carboxylic acid groups of polymers surrounding the emissive Ag NCs. Glutathione-capped Au NCs were also employed in a Cu^{2+} chemosensor application based on aggregation-induced fluorescence quenching [101]. This assay possesses a good selectivity toward Cu^{2+} over other metal ions, with a LOD of 3.6 nM. Moreover, the Cu^{2+}-quenched fluorescence could be efficiently recovered upon addition of a metal ion chelator, ethylenediaminetetraacetate (EDTA). Because these turn-off assays may compromise specificity since other quenchers or environmental stimulus might also lead to fluorescence quenching and report ''false positive'' results, Chang and coworkers [102] recently demonstrated a novel, turn-on fluorescent assay for Cu^{2+} using DNA-templated Ag NCs. The introduction of Cu^{2+} resulted in the formation of DNA—Cu/Ag NCs with more complete protection from DNA templates and thus enhanced the fluorescence. Furthermore, by using a combination of DNA-Cu/Ag NCs and 3-mercaptopropionic acid (MPA), they observed that MPA-induced fluorescence quenching of DNA-Cu/Ag NCs was suppressed in the presence of Cu^{2+} ions, allowing turn-on detection of Cu^{2+} at concentrations as low as 2.7 nM [103]. Fluorescence assays in the NIR region possess many advantages over visible fluorescence, which is particularly attractive for sensitive in vivo determination of biological targets [104]. Guo et al. [105] recently presented a NIR fluorescent assay for Cu^{2+} based on the quenching of luminescent Au NCs prepared via heat-assisted reduction of a gold(I)-thiol complex. This NIR fluorescence-based method enabled the sensitive detection of Cu^{2+} with a LOD down to 1.6 nM.

Detection of small biomolecules

Biothiols such as cysteine (Cys), homocysteine (Hcy) and glutathione (GSH) play a critical role in reversible redox reactions and important cellular functions including detoxification and metabolism. The analysis of their levels in human body fluids plays an important role in the early diagnosis of many diseases [106]. A simple fluorescence method for Cys detection has been developed based on PMAA-Ag NCs [107]. The fluorescence of Ag NCs can be efficiently quenched by Cys rather than other α-amino acids, which allowed the selective determination of Cys with a LOD of 20 nM. Based on the absorption and fluorescence, these researchers suggested that Cys quenched the fluo-

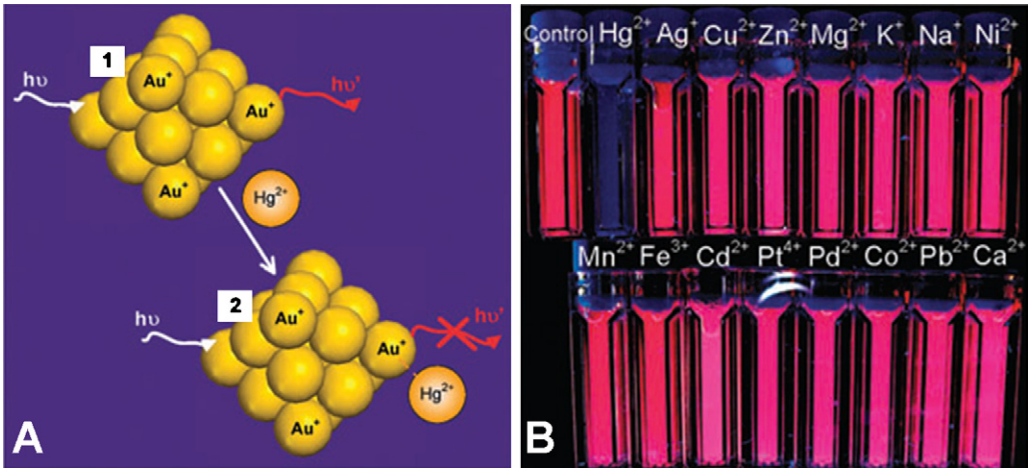

Fig. 8 (A) Schematic representation of Hg^{2+} sensing based on fluorescence quenching of Au NCs resulting from high-affinity metallophilic Hg^{2+}—Au^{+} bonds. (B) Photographs of aqueous BSA-Au NCs solutions (20 μM) in the presence of 50 μM of various metal ions under UV light.
(Reprinted with permission from Ref. [97] ©2010 the Royal Society of Chemistry.)

rescence by thiol-adsorption-accelerated oxidation of the fluorescent Ag clusters. Oligonucleotide-stabilized Ag NCs have also been demonstrated to be capable of detecting biothiols [108]. The sensing mechanism was based on fluorescence quenching due to formation of non-fluorescent complexes between DNA-Ag NCs and biothiols. The detection limits for Cys, Hcy and GSH were measured to be 4.0 nM, 4.0 nM and 200 nM, respectively. By virtue of the template-dependent fluorescence properties of DNA-Ag NCs and their specific response to thiol compounds, Qu and coworkers [109] recently introduced a novel fluorescent turn-on assay for biothiols with high specificity and sensitivity. Contrary to previous work, which reported fluorescence quenching of Ag NCs by biothiols, they found that the emission of some DNA-Ag NCs such as those with 12 cytosines could be enhanced in the presence of thiol compounds (Fig. 9). This turn-on assay enabled a sensitive determination of GSH with a LOD as low as 6.2 nM, which was at least a magnitude lower than the previous turn-off assay [108]. This study also showed that Ag NCs formed in different DNA templates could have different fluorescence response patterns to analytes, suggesting the opportunity to modulate the response patterns of DNA-Ag NCs to a specific analyte simply by selecting appropriate DNA templates in nanocluster synthesis.

Hydrogen peroxide (H_2O_2) represents another example of an analyte attracting a great deal of attention due to its involvement in many chemical, biological, pharmaceutical and environmental processes. Particularly, H_2O_2 is one of the products of enzymatic reactions by almost all oxidases, thus enabling quantitative assays of the activity of the enzyme as well as various enzyme substrates such as glucose [110,111]. Chang et al. [112] developed an assay system for the quantitative determination of H_2O_2 using fluorescent 11-MUA-Au NCs based on luminescence quenching. In the presence of H_2O_2, 11-MUA units bound to the cluster surface through Au—S bonds are readily oxidized to form an organic disulfide product, resulting in reduced luminescence. This method was reported to detect H_2O_2 over a wide dynamic range (100 nM to 1.0 mM) with a LOD of 30 nM, comparable to other optical H_2O_2 sensors. Further combination of luminescent

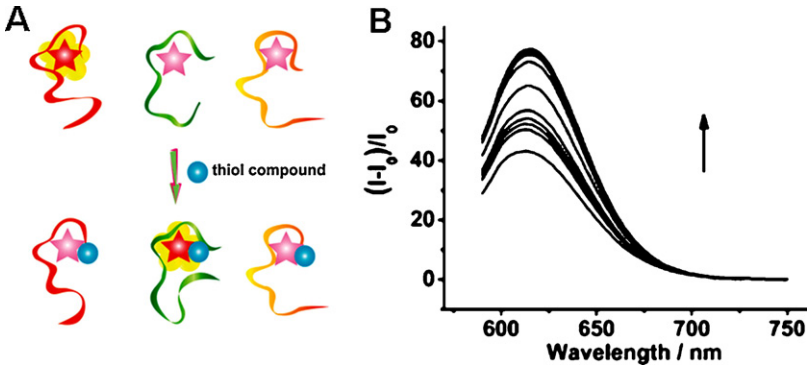

Fig. 9 (A) Schematic illustration of the template-dependent fluorescence response patterns of different DNA-Ag NCs to thiol compounds. (B) Representative fluorescence spectra of dC12-Ag NCs in the presence of increasing glutathione concentrations (0—2000 nM).
(Reprinted with permission from Ref. [109] ©2011 the Royal Society of Chemistry.)

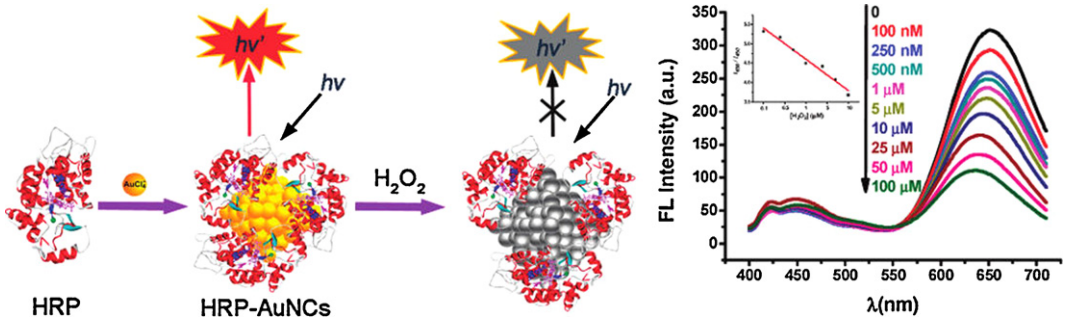

Fig. 10 (Left) Schematic representation of the formation of HRP-Au NCs and the H_2O_2-induced quenching. (Right) Fluorescence response of HRP-Au NCs after adding H_2O_2 (0—100 μM). Inset: Plot of the fluorescence ratio [I_{650}/I_{450}] of HRP-Au NCs versus the log concentration of H_2O_2.
(Reprinted with permission from Ref. [75] ©2011 American Chemical Society.)

Au NCs with glucose oxidase enabled the sensitive determination of glucose. Dong and coworkers [113] demonstrated that BSA-stabilized Au NCs could also be utilized for the facile detection of glucose with a LOD of 5.0 μM. The sensing mechanism was based on the enzymatically generated H_2O_2-induced degradation of Au NCs, which resulted in the fluorescence quenching. Zhang et al. [75] recently reported a new strategy to construct enzyme-functionalized fluorescent Au NCs for the detection of H_2O_2 (Fig. 10). Bifunctional fluorescent Au NCs could be formed in situ using horseradish peroxidase (HRP) as a scaffold. The enzyme remains active in the clusters and enables the catalytic reaction of HRP-Au NCs and H_2O_2, resulting in the fluorescence quenching that can be applied to H_2O_2 detection with high sensitivity (LOD: 30 nM).

Detection of proteins

Conjugation of selective receptor molecules (e.g. antibodies and aptamers) to the surface of fluorescent metal NCs has been employed for the development of metal NC-based fluorescent protein sensors. The first application of fluorescent metal NCs for protein detection was reported in 2006 by Leblanc et al. [114]. The polyclonal, goat-derived anti-human IgG antibody was electrostatically conjugated with PAMAM dendrimer-encapsulated Au NCs to construct a human IgG immunoassay. The system was able to detect IgG by linear fluorescence quenching in response to changes in the surface electrostatic properties of Au NCs by the formation of antigen—antibody immunocomplexes. Using fluorescent Au NCs as fluorophores and 13-nm Au nanoparticles (Au NPs) as quenchers, Chang and coworkers [115] developed a competitive fluorescence quenching assay for analyzing proteins (Fig. 11). Platelet-derived growth factor AA (PDGF AA) molecules were conjugated to 11-MUA-Au nanodots through electrostatic and hydrophobic interactions (denoted as PDGF AA-$L_{Au\ ND}$), and thiol-derivatized aptamers with high affinity toward PDGFs were modified on the surface of Au NPs (denoted as Apt-Q_{AuNP}). The fluorescence of PDGF AA-$L_{Au\ ND}$ decreased when fluorescence quenching occurred between Apt-Q_{AuNP} and PDGF AA-$L_{Au\ ND}$. The fluorescence quenching was efficiently suppressed in the presence of PDGF or PDGF α-receptor due to competitive reactions between them and Apt-Q_{AuNP}, which can be used as a turn-on fluorescence assay of PDGFs or PDGF receptors. The system allowed the detection of PDGF at concentrations as low as 0.5 nM in the presence of BSA at 10 μM. The same group also reported the utilization of biofunctional Au NCs as fluorescence sensors for the sensitive detection of other proteins including concanavalin A [116] and immunoglobulin G [117].

A straightforward method for the rapid detection of glutathione S-transferase (GST)-tagged proteins from cell lysates has been developed by Chen et al. [118] by using glutathione-stabilized Au NCs. The presence of GST-tagged proteins could be visualized under UV light illumination upon centrifugation of their conjugates with luminescent GSH-Au NCs. The LOD of this approach by simple observation with the naked eye was estimated to be 0.75 μM, which was slightly higher than the detection limit by using fluorescence spectroscopy (0.25 μM). Martinez and

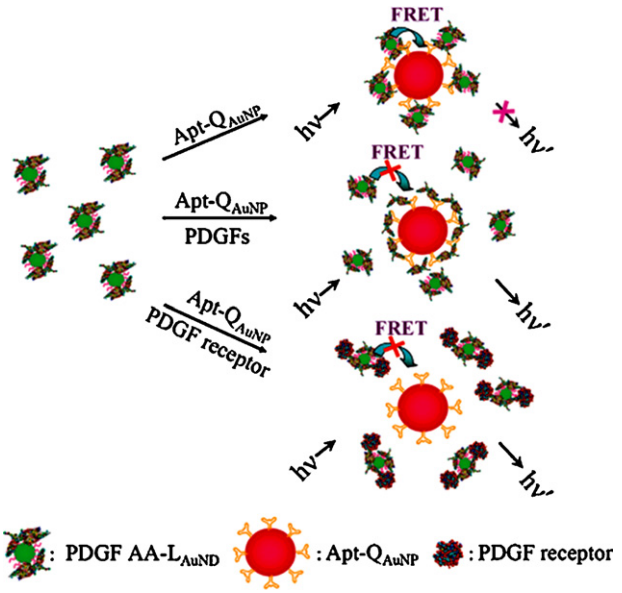

Fig. 11 Schematic representations of PDGF and PDGF receptor nanosensors based on the modulation of the fluorescence quenching between PDGF AA-L_{AuND} and Apt-Q_{AuNP}.
(Reprinted with permission from Ref. [115] ©2008 American Chemical Society.)

coworkers [119] recently developed a new strategy for detecting specific proteins using an intrinsically fluorescent recognition ligand that combines the high fluorescence QY (>50%) of oligonucleotide-templated Ag NCs with the specificity and strong binding affinity of DNA aptamers for their target proteins. This simple method was characterized by the simultaneous achievement of synthesizing fluorescent Ag NCs and conjugating the recognition molecules (aptamers) within one step. Further incorporating palettes of nanocluster-templating sequences, each with different fluorescence features and different aptamer sequences, would allow the development of multiplex protein detection schemes.

Detection of nucleic acids

Formation of fluorescent metal NCs can depend upon a number of factors, including solvent chemistry, pH and the scaffold. For instance, the emission properties of DNA-Ag NCs may vary greatly depending on the local environment and nucleotide sequences, which have recently been exploited as a new signal transduction mechanism for nucleic acid detection. By virtue of the highly sequence-dependent generation of fluorescent Ag NCs in hybridized DNA duplex scaffolds, Wang and coworkers [120] developed a new Ag NCs-based fluorescent assay capable of specifically identifying single nucleotide modifications in DNA. Their study showed that even a single-nucleotide mismatch located two bases away from the nanocluster formation site would prohibit the generation of fluorescent Ag NCs. As an example, they demonstrated the capability of this strategy to identify the sickle cell anemia mutation in the hemoglobin beta chain (HBB) gene.

On the basis of the finding that the red fluorescence of DNA-Ag NCs could be enhanced up to 500-fold when placed in proximity to guanine-rich DNA sequences, Yeh et al. [121] recently designed a DNA detection probe that ''lights up'' upon target binding. As shown in Fig. 12, dark DNA-Ag NCs can be transformed into bright red-emitting clusters when placed in proximity of guanine bases, which enabled the specific detection of DNA targets in a separation-free format. Particularly, this new type of nanocluster probe was able to detect the target with an extremely high signal-to-background ratio of 175, which is a factor of 5 better than by using a conventional molecular beacon probe.

Chang et al. [122] presented a one-pot synthesis of fluorescent and functional DNA-Ag NCs that act as selective and sensitive probes for DNA detection. The specific DNA scaffold combined a DNA sequence for the recognition of target DNA and a scaffold for the preparation of fluorescent Ag NCs. The detection was based on the different stabilities (read out by fluorescence intensities) of formed Ag NCs in solutions containing 0.15 M NaCl in the absence and presence of perfectly matching DNA, which allowed the sensitive detection of a gene for fumarylacetoacetate hydrolase (FAH) with a LOD of 14 nM.

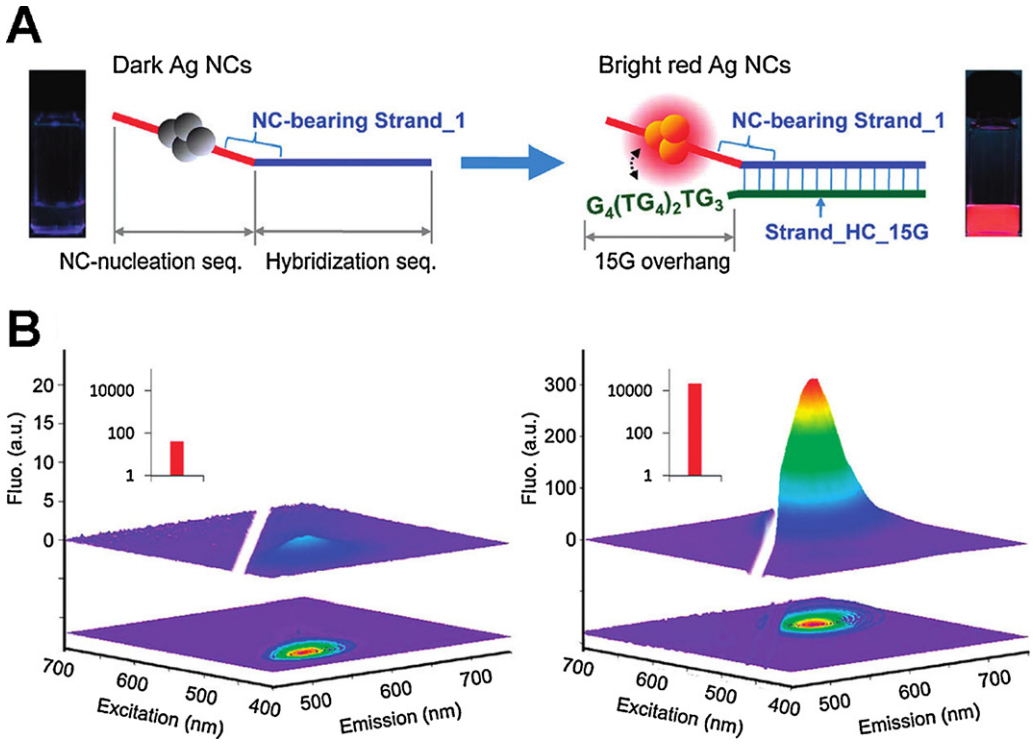

Fig. 12 (A) Schematic representation showing red fluorescence enhancement of DNA-Ag NCs through proximity with a G-rich overhang, 3′-$G_4(TG_4)_2TG_3$, caused by DNA hybridization and photographs of the resulting emission under UV (366 nm) irradiation. (B) 3D- and 2D-contour plots of excitation/emission spectra of the Ag NCs before (left) and after (right) hybridizing NC-bearing Strand_1 with Strand_HC_15G. Inset: Integrated red fluorescence emission with the buffer fluorescence subtracted in arbitrary units, which shows an enhancement of ~500-fold after duplex formation.
(Reprinted with permission from Ref. [121] ©2010 American Chemical Society.)

Application of fluorescent metal nanoclusters in biological imaging

Fluorescence imaging offers unique advantages over other imaging modalities in regard to sensitivity, multiplex detection capabilities and equipment cost. It relies heavily on stable, biocompatible, highly specific and sensitive markers [123]. Conventional fluorophores for imaging applications include organic dyes and engineered fluorescent proteins, which have limited photostability that can be a disadvantage for long-term experiments in live cells with high sensitivity. Semiconductor QDs have been considered as a promising alternative owing to their excellent photophysical properties such as good photostability and high fluorescence brightness; therefore, they have been under intense investigation for in vitro and in vivo imaging [5]. However, these QDs have prompted potential safety concerns for in vivo use. In addition, their larger dimensions, typically comparable to or larger than the size of proteins, could possibly affect the function of attached ligand molecules [3]. In contrast, fluorescent metal NCs are smaller and exhibit bright emission and good biocompatibility, making them attractive alternatives as fluorescent probes for bioimaging.

A number of papers have reported biological imaging applications based on fluorescent metal NCs. In an early report, Baskakov and coworkers [124] presented the first imaging application of Ag NCs in combination with a fluorophore, thioflavin T (ThT). Fluorescent NCs were generated in situ by sensitized photoreduction of Ag^+ in the presence of ThT. Notably, these hybrid NCs displayed ultrabright fluorescence in aqueous solution without any detectable photobleaching, and could be easily detected using a fluorescence microscope. The potential of these luminescent NCs for bioimaging was demonstrated by staining amyloid fibrils (Fig. 13). After incubation for 5 min with preformed ThT-Ag NCs, amyloid fibrils were observed to be covered by blinking fluorescent clusters. Whereas amyloid fibrils stained with ThT-Ag NCs displayed a time-dependent increase of fluorescence with no appreciable photobleaching even after 24 h of illumination at 475 nm (500 W/cm^2), those stained only with ThT showed a rapid decay of the fluorescence and were barely detectable even after 1 min of illumination.

Dickson and coworkers [67] reported the staining of living cells by intracellularly generated, fluorescent peptide-encapsulated Ag NCs. These ultrasmall Ag NCs were found to distribute evenly within the cells and some even passed through the nuclear membrane, resulting in a weak nuclear staining. Because these Ag NCs exhibited short lifetimes (220 ps (33%) and 1760 ps (67%)), they could be monitored with time-gated microscopy to minimize contributions from autofluorescence or other co-loaded dyes with slower emission. Later, the same group reported the application of fluorescent DNA-Ag NCs to biological imaging in a more specific way through surface labeling of live cells [125]. These DNA-Ag NCs were readily conjugated with proteins such as avidin without significantly perturbing their biological function, owing to the ultrasmall size of Ag NCs. Employing simple avidin—biotin interactions, avidin-conjugated Ag NCs could stain the cell surface and be internalized. Moreover, in recent studies, metal NCs were delivered into living cells by microinjection [126], conjugation with a cell penetrating peptide [126—128], using a transfection agent [129], or simple endocytosis [29,42], thereby opening strategies toward intracellular labeling and imaging.

Two-photon imaging can be advantageous for the study of biological samples because of the ability of deeper imaging inside tissues and the reduced phototoxicity of NIR light. The outstanding TPA cross sections of metal NCs make them good candidates for application in two-photon cellular imaging. Using dextran-encapsulated 11-MUA-Au NCs as the fluorophore, Chou and coworkers [88] investigated their potential for two-photon imaging of human mesenchymal stem cells (hMSCs). Bright luminescence from Au NCs could be observed in fixed cell samples via two-photon excitation in a confocal microscope using 800 nm laser pulses, thus validating the applicability of fluorescent Au NCs in two-photon imaging. Xu et al. [89] also presented applications of glutathione-protected Au NCs, which possess a much higher TPA cross section than 11-MUA-Au NCs, for two-photon excitation in live cell imaging. Recently, Nienhaus and coworkers [29] investigated the internalization of fluorescent DPA-Au NCs by live HeLa cells via two-photon fluorescence imaging. After incubation with DPA-Au NCs for 2 h, cells were imaged by using confocal microscopy with TPE at 810 nm. As shown in Fig. 14, the bright luminescence from clusters of ingested NCs could easily be observed inside the cells. Cells were also imaged at different z-positions for 3D reconstruction, which revealed DPA-Au NCs inside the cells as well as

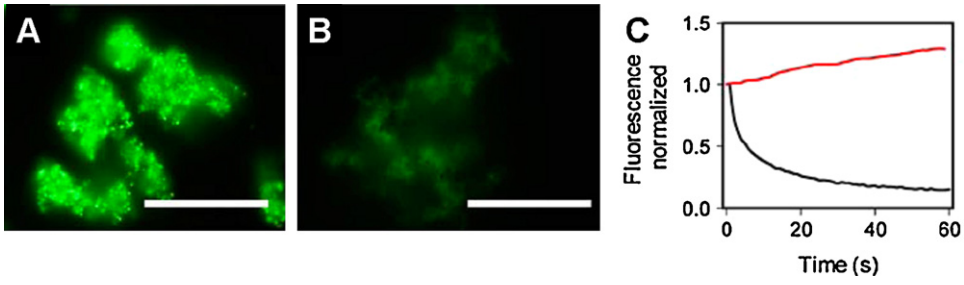

Fig. 13 Epifluorescence microscopy images of amyloid fibrils of PrP 90—231 stained with (A) preformed ThT-Ag NCs and (B) 10 μM ThT, respectively. Scale bars: 10 μm. ThT-Ag NCs were generated by the irradiation of aqueous solutions containing ThT (10 μM) and $AgNO_3$ (1 μM) at 312 nm for 3 min. (C) Photobleaching kinetics of the fibrils stained with ThT (black line) versus photoactivation kinetics of the fibrils stained with ThT-Ag NCs (red line). The kinetics were collected from a 5 μm × 5 μm area and normalized to the intensity measured at zero time.
(Reprinted with permission from Ref. [124] ©2005 Elsevier.)

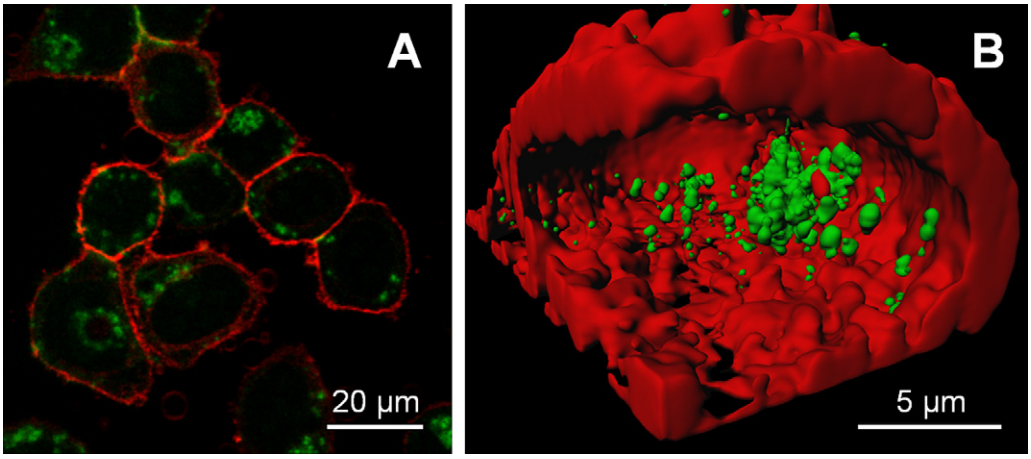

Fig. 14 (A) Fluorescence image, taken with 810 nm two-photon excitation after incubation of HeLa cells with DPA-Au NCs (100 μg/ml) for 2 h. (B) Cross section of a 3D image reconstruction, showing internalized DPA-Au NCs. Membranes were stained with the red dye DiD.

attached to the membrane. While elucidating the detailed uptake mechanism of these ultrasmall Au NCs still requires more investigation, the finding that most particles inside the cells existed in the form of large aggregates suggests they were taken up by specific endocytosis pathways that package a large number of particles into endosomal vesicles [130].

Wu et al. [131] recently presented the first example of in vivo fluorescence imaging in animals with ultrasmall BSA-stabilized Au NCs. The fluorescence signal of Au NCs in living organisms could be spectrally distinguished from the background, and the high photostability as well as the low toxicity of Au NCs indicated their potential for continuous imaging in vivo. As shown in Fig. 15, fluorescence images of the subcutaneously injected mice exhibited bright emission from different locations depending on the injected Au NC dose. The fluorescence of Au NCs could also be visualized upon injection into muscles by up to a few millimeters, owing to the improved tissue penetration afforded by NIR fluorescence. Au NCs were intravenously injected into athymic nude mice and subjected to whole body real-time in vivo imaging. Immediately after tail vein injection, the fluorescence from Au NCs-injected mice was easily visualized in the superficial vasculature of the whole body. The fluorescence signals remained visible in the circulation even at 5 h post injection, and decreased noticeably 24 h post injection. Furthermore, using two different tumor models, in vivo and ex vivo imaging studies showed that the ultrasmall Au NCs could be accumulated to a high level in tumor sites owing to the enhanced permeability and retention (EPR) effects. Recent work by Zheng et al. found that the renal clearance of 2 nm glutathione-coated luminescent Au NCs was more than 10—100 times better than that of similarly sized nonluminescent Au NPs [132]. The small size

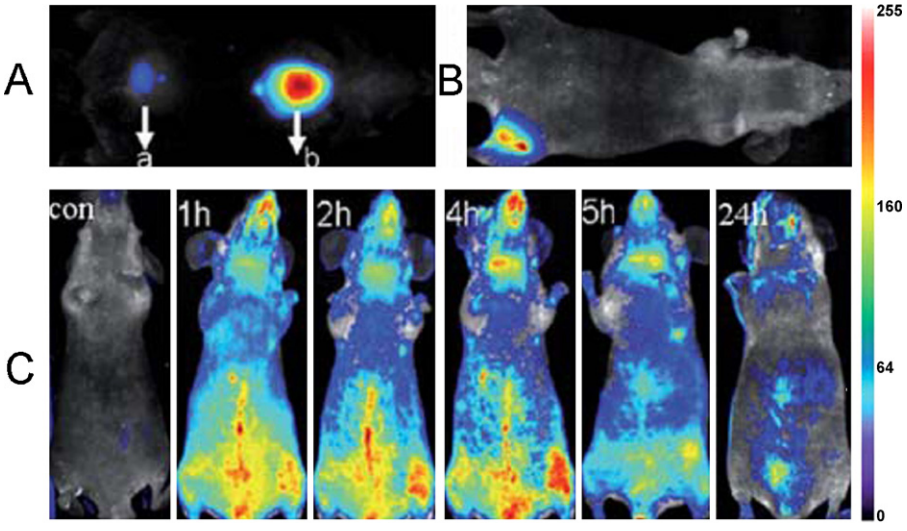

Fig. 15 In vivo fluorescence image of 100 μl Au NCs injected (A) subcutaneously (a: 0.235 mg ml^{-1}, b: 2.35 mg ml^{-1}) and (B) intramuscularly (2.35 mg ml^{-1}) into mice. (C) Real-time in vivo abdomen imaging upon intravenous injection with 200 μl of Au NCs (2.35 mg ml^{-1}) at different time points post injection.
(Reprinted with permission from Ref. [131] ©2010 the Royal Society of Chemistry.)

in combination with surface ligands not only enables the majority of the luminescent Au NCs to be cleared from the body through kidney filtration, but also stabilizes the luminescent Au NCs during blood circulation. This variety of studies has clearly demonstrated that ultrasmall NIR Au NCs are promising contrast imaging agents for in vivo fluorescence imaging.

Summary and perspective

Fluorescent metal NCs are a novel class of luminescent nanomaterials. Their attractive properties including ultrasmall size, low toxicity, lack of intermittency and low photobleaching make them attractive fluorescent probes for biological applications. Recent advances in the synthesis of fluorescent Au/Ag NCs by a variety of approaches have contributed significantly to progress toward a fundamental understanding of their fascinating optical properties as well as the development of applications in bioanalysis and biological imaging. Despite their great potential and promising future as novel labeling agents, further advancement of fluorescent metal NCs faces a variety of challenges.

First, there remains a good deal of room for developing better synthesis routes to produce high quality metal NCs. Particularly, most of the currently reported metal NCs possess a relatively low QY (less than 10%) in comparison to semiconductor QDs and many organic dyes. In addition, NCs often show size heterogeneity in the crude product. Polydispersity definitely compromises their attractiveness as fluorophores and also makes detailed fundamental studies of their properties (such as structure determination and quantification) more difficult. Thus, it is an important goal to develop new synthesis strategies to efficiently produce monodisperse, bright metal NCs. In this regard, Jin et al. [133] recently demonstrated the possibility of synthesizing atomically monodisperse thiol-functionalized Au_{25} NCs. They also revealed that ligands with electron-rich atoms or groups can markedly enhance the fluorescence of Au NCs [19]. This observation may spawn new strategies for future progress in this direction.

Second, in addition to fluorescence, it could be useful to simultaneously endow metal NCs with other properties. Such bi- or multifunctional probes bear a lot of promise for applications. Especially, magnetic nanomaterials exhibit a unique magnetic resonance (MR) contrast enhancement effect that enables noninvasive MR imaging of cell trafficking, gene expression and cancer [134]. For clinical applications requiring in vivo imaging, probes comprising fluorescence and magnetism can be advantageous because of their ability to be detected optically and magnetically. Another possibility could be to combine fluorescent metal NCs with plasmonic materials such as gold, which may yield unique multifunctional nanoprobes for plasmon and fluorescence-based imaging and detection [135]. The rational design and fabrication of such multifunctional metal NC-based probes can be very challenging. The recent success in coating Au NCs with silica may likely assist in this endeavor, owing to the possibility of introducing different functionalities on the silica surface [136,137].

Third, despite many reports on the biological application of fluorescent metal NCs, relatively little is known about the interaction of these ultra-small clusters with the biological environment. For instance, in a biological fluid, proteins can adsorb and associate with nanoparticles, which can have significant impact on the biological behavior of both proteins and nanoparticles [138,139]. Correspondingly, a better understanding of the interactions between metal NCs and proteins and other biomolecules is important to understand the mechanistic basis of the biological activity of these NCs and to make safe use of nanotechnology. Moreover, it would be also interesting to explore the fate of these tiny clusters after entering live cells, i.e., where do they go, do they change cell signaling or other cellular properties, or how are they processed and degraded by the cells?

In conclusion, fluorescent metal NCs have attractive features for their application as ultrasmall biocompatible labels. As the synthesis and biological applications of these fluorescent metal NCs are still at an early stage, much work remains to be done before these clusters will be widely employed as alternatives to conventional fluorophores in practical applications. With further advances in design and synthesis of high quality, multifunctional metal NCs, we expect their widespread application in advanced image-guided therapy, intracellular drug delivery, ultrasensitive molecular diagnostics, as well as novel light-emitting nanodevices over the years to come.

Acknowledgements

This work was supported by the Deutsche Forschungsgemeinschaft (DFG) through the Center for Functional Nanostructures (CFN) and the Priority Program SPP1313. L.S. gratefully acknowledges support from the Alexander von Humboldt (AvH) Foundation.

References

[1] M.C. Roco, Curr. Opin. Biotechnol. 14 (2003) 337—346.
[2] Y.C. Cao, Nanomedicine 3 (2008) 467—469.
[3] F. Wang, W.B. Tan, Y. Zhang, X. Fan, M. Wang, Nanotechnology 17 (2006) R1.
[4] M. Baker, Nat. Methods 7 (2010) 957—962.
[5] X. Michalet, F. Pinaud, L. Bentolila, J. Tsay, S. Doose, J. Li, G. Sundaresan, A. Wu, S. Gambhir, S. Weiss, Science 307 (2005) 538—544.
[6] J. Yan, M.C. Estévez, J.E. Smith, K. Wang, X. He, L. Wang, W. Tan, Nano Today 2 (2007) 44—50.
[7] D.K. Chatterjee, M.K. Gnanasammandhan, Y. Zhang, Small 6 (2010) 2781—2795.
[8] S.N. Baker, G.A. Baker, Angew. Chem. Int. Ed. 49 (2010) 6726—6744.
[9] G.U. Nienhaus, Angew. Chem. Int. Ed. 47 (2008) 8992—8994.
[10] J. Zheng, P.R. Nicovich, R.M. Dickson, Ann. Rev. Phys. Chem. 58 (2007) 409—431.
[11] H. Xu, K.S. Suslick, Adv. Mater. 22 (2010) 1078—1082.
[12] I. Diez, R.H.A. Ras, Nanoscale 3 (2011) 1963—1970.
[13] M.A.H. Muhammed, T. Pradeep, in: A.P. Demchenko (Ed.), Advanced Fluorescence Reporters in Chemistry and Biology II, Springer, Berlin, Heidelberg, 2010, pp. 333—353.
[14] I. Díez, R. Ras, Advanced Fluorescence Reporters in Chemistry and Biology II, Springer, 2010, pp. 307—332.
[15] C. Lin, C. Lee, J. Hsieh, H. Wang, J. Li, J. Shen, W. Chan, H. Yeh, W. Chang, J. Med. Biol. Eng. 29 (2009) 276—283.

[16] W. Wei, Y. Lu, W. Chen, S. Chen, J. Am. Chem. Soc. 133 (2011) 2060—2063.
[17] S.-I. Tanaka, J. Miyazaki, D.K. Tiwari, T. Jin, Y. Inouye, Angew. Chem. Int. Ed. 50 (2011) 431—435.
[18] A. Mooradian, Phys. Rev. Lett. 22 (1969) 185—187.
[19] Z. Wu, R. Jin, Nano Lett. 10 (2010) 2568—2573.
[20] R. Jin, Nanoscale 2 (2010) 343—362.
[21] S. Link, A. Beeby, S. FitzGerald, M. El-Sayed, T. Schaaff, R. Whetten, J. Phys. Chem. B 106 (2002) 3410—3415.
[22] Y. Negishi, K. Nobusada, T. Tsukuda, J. Am. Chem. Soc. 127 (2005) 5261—5270.
[23] Y. Negishi, Y. Takasugi, S. Sato, H. Yao, K. Kimura, T. Tsukuda, J. Am. Chem. Soc. 126 (2004) 6518—6519.
[24] T. Huang, R. Murray, J. Phys. Chem. B 105 (2001) 12498—12502.
[25] D. Lee, R.L. Donkers, G. Wang, A.S. Harper, R.W. Murray, J. Am. Chem. Soc. 126 (2004) 6193—6199.
[26] M. Paau, C. Lo, X. Yang, M. Choi, J. Phys. Chem. C 114 (2010) 15995—16003.
[27] Z. Wang, W. Cai, J. Sui, ChemPhysChem 10 (2009) 2012—2015.
[28] B. Adhikari, A. Banerjee, Chem. Mater. 22 (2010) 4364—4371.
[29] L. Shang, R.M. Dörlich, S. Brandholt, R. Schneider, V. Trouillet, M. Bruns, D. Gerthsen, G.U. Nienhaus, Nanoscale 3 (2011) 2009—2014.
[30] C.-C. Huang, Z. Yang, K.-H. Lee, H.-T. Chang, Angew. Chem. Int. Ed. 46 (2007) 6824—6828.
[31] C.-C. Huang, H.-Y. Liao, Y.-C. Shiang, Z.-H. Lin, Z. Yang, H.-T. Chang, J. Mater. Chem. 19 (2009) 755—759.
[32] C.-C. Huang, Y.-L. Hung, Y.-C. Shiang, T.-Y. Lin, Y.-S. Lin, C.-T. Chen, H.-T. Chang, Chem. Asian J. 5 (2010) 334—341.
[33] M. Habeeb Muhammed, S. Ramesh, S. Sinha, S. Pal, T. Pradeep, Nano Res. 1 (2008) 333—340.
[34] M. Muhammed, P. Verma, S. Pal, R. Kumar, S. Paul, R. Omkumar, T. Pradeep, Chem. Eur. J. 15 (2009) 10110—10120.
[35] C.A. Lin, T.Y. Yang, C.H. Lee, S.H. Huang, R.A. Sperling, M. Zanella, J.K. Li, J.L. Shen, H.H. Wang, H.I. Yeh, W.J. Parak, W.H. Chang, ACS Nano 3 (2009) 395—401.
[36] T. Udaya Bhaskara Rao, T. Pradeep, Angew. Chem. Int. Ed. 49 (2010) 3925—3929.
[37] T.U.B. Rao, B. Nataraju, T. Pradeep, J. Am. Chem. Soc. 132 (2010) 16304—16307.
[38] J. Zheng, R.M. Dickson, J. Am. Chem. Soc. 124 (2002) 13982—13983.
[39] J. Zheng, J.T. Petty, R.M. Dickson, J. Am. Chem. Soc. 125 (2003) 7780—7781.
[40] J. Zheng, C. Zhang, R.M. Dickson, Phys. Rev. Lett. 93 (2004) 077402.
[41] Y.P. Bao, C. Zhong, D.M. Vu, J.P. Temirov, R.B. Dyer, J.S. Martinez, J. Phys. Chem. C 111 (2007) 12194—12198.
[42] Y.-C. Jao, M.-K. Chen, S.-Y. Lin, Chem. Commun. 46 (2010) 2626—2628.
[43] J.G. Zhang, S.Q. Xu, E. Kumacheva, Adv. Mater. 17 (2005) 2336—2340.
[44] Z. Shen, H.W. Duan, H. Frey, Adv. Mater. 19 (2007) 349—352.
[45] L. Shang, S.J. Dong, Chem. Commun. (2008) 1088—1090.
[46] I. Díez, M. Pusa, S. Kulmala, H. Jiang, A. Walther, A.S. Goldmann, A.H.E. Muller, O. Ikkala, R.H.A. Ras, Angew. Chem. Int. Ed. 48 (2009) 2122—2125.
[47] H. Xu, K.S. Suslick, ACS Nano 4 (2010) 3209—3214.
[48] S. Liu, F. Lu, J.-J. Zhu, Chem. Commun. 47 (2011) 2661—2663.
[49] H. Duan, S. Nie, J. Am. Chem. Soc. 129 (2007) 2412—2413.
[50] N. Schaeffer, B. Tan, C. Dickinson, M.J. Rosseinsky, A. Laromaine, D.W. McComb, M.M. Stevens, Y. Wang, L. Petit, C. Barentin, D.G. Spiller, A.I. Cooper, R. Levy, Chem. Commun. (2008) 3986—3988.
[51] B. Santiago González, M.a.J. Rodríguez, C. Blanco, J. Rivas, M.A. Lòpez-Quintela, J.M.G. Martinho, Nano Lett. 10 (2010) 4217—4221.
[52] H. Yabu, Chem. Commun. 47 (2011) 1196—1197.
[53] S. Pitchiaya, Y. Krishnan, Chem. Soc. Rev. 35 (2006) 1111—1121.
[54] N. Dattagupta, D.M. Crothers, Nucl. Acids Res. 9 (1981) 2971—2985.
[55] K.F.S. Luk, A.H. Maki, R.J. Hoover, J. Am. Chem. Soc. 97 (1975) 1241—1242.
[56] J.T. Petty, J. Zheng, N.V. Hud, R.M. Dickson, J. Am. Chem. Soc. 126 (2004) 5207—5212.
[57] T. Vosch, Y. Antoku, J.C. Hsiang, C.I. Richards, J.I. Gonzalez, R.M. Dickson, Proc. Natl. Acad. Sci. U.S.A. 104 (2007) 12616—12621.
[58] C.M. Ritchie, K.R. Johnsen, J.R. Kiser, Y. Antoku, R.M. Dickson, J.T. Petty, J. Phys. Chem. C 111 (2007) 175—181.
[59] B. Sengupta, C.M. Ritchie, J.G. Buckman, K.R. Johnsen, P.M. Goodwin, J.T. Petty, J. Phys. Chem. C 112 (2008) 18776—18782.
[60] E.G. Gwinn, P. O'Neill, A.J. Guerrero, D. Bouwmeester, D.K. Fygenson, Adv. Mater. 20 (2008) 279—283.
[61] B. Sengupta, K. Springer, J.G. Buckman, S.P. Story, O.H. Abe, Z.W. Hasan, Z.D. Prudowsky, S.E. Rudisill, N.N. Degtyareva, J.T. Petty, J. Phys. Chem. C 113 (2009) 19518—19524.
[62] J. Sharma, H.-C. Yeh, H. Yoo, J.H. Werner, J.S. Martinez, Chem. Commun. 46 (2010) 3280—3282.
[63] C.I. Richards, S. Choi, J.C. Hsiang, Y. Antoku, T. Vosch, A. Bongiorno, Y.L. Tzeng, R.M. Dickson, J. Am. Chem. Soc. 130 (2008) 5038—5039.
[64] P.R. O'Neill, L.R. Velazquez, D.G. Dunn, E.G. Gwinn, D.K. Fygenson, J. Phys. Chem. C 113 (2009) 4229—4233.
[65] Z. Huang, F. Pu, D. Hu, C. Wang, J. Ren, X. Qu, Chem. Eur. J. 17 (2011) 3774—3780.
[66] R. Zhou, M. Shi, X. Chen, M. Wang, H. Chen, Chem. Eur. J. 15 (2009) 4944—4951.
[67] J. Yu, S.A. Patel, R.M. Dickson, Angew. Chem. Int. Ed. 46 (2007) 2028—2030.
[68] B. Adhikari, A. Banerjee, Chem. Eur. J. 16 (2010) 13698—13705.
[69] J. Xie, Y. Zheng, J.Y. Ying, J. Am. Chem. Soc. 131 (2009) 888—889.
[70] H. Wei, Z. Wang, L. Yang, S. Tian, C. Hou, Y. Lu, Analyst 135 (2010) 1406—1410.
[71] P.L. Xavier, K. Chaudhari, P.K. Verma, S.K. Pal, T. Pradeep, Nanoscale 2 (2010) 2769—2776.
[72] X.L. Guével, N. Daum, M. Schneider, Nanotechnology 22 (2011) 275103.
[73] C. Guo, J. Irudayaraj, Anal. Chem. 83 (2011) 2883—2889.
[74] M.A. Habeeb Muhammed, P.K. Verma, S.K. Pal, A. Retnakumari, M. Koyakutty, S. Nair, T. Pradeep, Chem. Eur. J. 16 (2010) 10103—10112.
[75] F. Wen, Y. Dong, L. Feng, S. Wang, S. Zhang, X. Zhang, Anal. Chem. 83 (2011) 1193—1196.
[76] S.S. Narayanan, S.K. Pal, J. Phys. Chem. C 112 (2008) 4874—4879.
[77] M. Zhu, C.M. Aikens, F.J. Hollander, G.C. Schatz, R. Jin, J. Am. Chem. Soc. 130 (2008) 5883—5885.
[78] B.N.G. Giepmans, S.R. Adams, M.H. Ellisman, R.Y. Tsien, Science 312 (2006) 217—224.
[79] J. Wiedenmann, G.U. Nienhaus, Expert Rev. Proteom. 3 (2006) 361—374.
[80] G.U. Nienhaus, J. Wiedenmann, ChemPhysChem 10 (2009) 1369—1379.
[81] T. Huang, R.W. Murray, J. Phys. Chem. B 107 (2003) 7434—7440.

[82] C. Zhou, C. Sun, M. Yu, Y. Qin, J. Wang, M. Kim, J. Zheng, J. Phys. Chem. C 114 (2010) 7727—7732.
[83] H. Chen, X. Kou, Z. Yang, W. Ni, J. Wang, Langmuir 24 (2008) 5233—5237.
[84] S.A. Patel, M. Cozzuol, J.M. Hales, C.I. Richards, M. Sartin, J.-C. Hsiang, T. Vosch, J.W. Perry, R.M. Dickson, J. Phys. Chem. C 113 (2009) 20264—20270.
[85] K.A. Willets, R.P. Van Duyne, Ann. Rev. Phys. Chem. 58 (2007) 267—297.
[86] P.T.C. So, C.Y. Dong, B.R. Masters, K.M. Berland, Annu. Rev. Biomed. Eng. 2 (2000) 399—429.
[87] G. Ramakrishna, O. Varnavski, J. Kim, D. Lee, T. Goodson, J. Am. Chem. Soc. 130 (2008) 5032—5033.
[88] C. Liu, M. Ho, Y. Chen, C. Hsieh, Y. Lin, Y. Wang, M. Yang, H. Duan, B. Chen, J. Lee, J. Phys. Chem. C 113 (2009) 21082—21089.
[89] L. Polavarapu, M. Manna, Q.-H. Xu, Nanoscale 3 (2011) 429—434.
[90] D.R. Larson, W.R. Zipfel, R.M. Williams, S.W. Clark, M.P. Bruchez, F.W. Wise, W.W. Webb, Science 300 (2003) 1434—1436.
[91] S.A. Patel, C.I. Richards, J.-C. Hsiang, R.M. Dickson, J. Am. Chem. Soc. 130 (2008) 11602—11603.
[92] X.-B. Yin, S. Dong, E. Wang, Trends Anal. Chem. 23 (2004) 432—441.
[93] R.J. Forster, P. Bertoncello, T.E. Keyes, Annu. Rev. Anal. Chem. 2 (2009) 359—385.
[94] Y.-M. Fang, J. Song, J. Li, Y.-W. Wang, H.-H. Yang, J.-J. Sun, G.-N. Chen, Chem. Commun. 47 (2011) 2369—2371.
[95] L. Li, H. Liu, Y. Shen, J. Zhang, J.-J. Zhu, Anal. Chem. 83 (2011) 661—665.
[96] P. Holmes, K.A.F. James, L.S. Levy, Sci. Total Environ. 408 (2009) 171—182.
[97] J. Xie, Y. Zheng, J.Y. Ying, Chem. Commun. 46 (2010) 961—963.
[98] Y.-H. Lin, W.-L. Tseng, Anal. Chem. 82 (2010) 9194—9200.
[99] W. Guo, J. Yuan, E. Wang, Chem. Commun. (2009) 3395—3397.
[100] L. Shang, S.J. Dong, J. Mater. Chem. 18 (2008) 4636—4640.
[101] W. Chen, X. Tu, X. Guo, Chem. Commun. (2009) 1736—1738.
[102] G.-Y. Lan, C.-C. Huang, H.-T. Chang, Chem. Commun. 46 (2010) 1257—1259.
[103] Y.-T. Su, G.-Y. Lan, W.-Y. Chen, H.-T. Chang, Anal. Chem. 82 (2010) 8566—8572.
[104] L. Shang, J. Yin, J. Li, L. Jin, S. Dong, Biosens. Bioelectron. 25 (2009) 269—274.
[105] X. Tu, W. Chen, X. Guo, Nanotechnology 22 (2011) 095701.
[106] X. Chen, Y. Zhou, X. Peng, J. Yoon, Chem. Soc. Rev. 39 (2010) 2120—2135.
[107] L. Shang, S. Dong, Biosens. Bioelectron. 24 (2009) 1569—1573.
[108] B. Han, E. Wang, Biosens. Bioelectron. 26 (2011) 2585—2589.
[109] Z. Huang, F. Pu, Y. Lin, J. Ren, X. Qu, Chem. Commun. 47 (2011) 3487—3489.
[110] L. Shang, H. Chen, L. Deng, S. Dong, Biosens. Bioelectron. 23 (2008) 1180—1184.
[111] L. Shang, S.J. Dong, Anal. Chem. 81 (2009) 1465—1470.
[112] Y.-C. Shiang, C.-C. Huang, H.-T. Chang, Chem. Commun. (2009) 3437—3439.
[113] L. Jin, L. Shang, S. Guo, Y. Fang, D. Wen, L. Wang, J. Yin, S. Dong, Biosens. Bioelectron. 26 (2011) 1965—1969.
[114] R.C. Triulzi, M. Micic, S. Giordani, M. Serry, W.-A. Chiou, R.M. Leblanc, Chem. Commun. (2006) 5068—5070.
[115] C.-C. Huang, C.-K. Chiang, Z.-H. Lin, K.-H. Lee, H.-T. Chang, Anal. Chem. 80 (2008) 1497—1504.
[116] C.-C. Huang, C.-T. Chen, Y.-C. Shiang, Z.-H. Lin, H.-T. Chang, Anal. Chem. 81 (2009) 875—882.
[117] Y.-C. Shiang, C.-A. Lin, C.-C. Huang, H.-T. Chang, Analyst 136 (2011) 1177—1182.
[118] C.-T. Chen, W.-J. Chen, C.-Z. Liu, L.-Y. Chang, Y.-C. Chen, Chem. Commun. (2009) 7515—7517.
[119] J. Sharma, H.-C. Yeh, H. Yoo, J.H. Werner, J.S. Martinez, Chem. Commun. 47 (2011) 2294—2296.
[120] W. Guo, J. Yuan, Q. Dong, E. Wang, J. Am. Chem. Soc. 132 (2010) 932—934.
[121] H.-C. Yeh, J. Sharma, J.J. Han, J.S. Martinez, J.H. Werner, Nano Lett. 10 (2010) 3106—3110.
[122] G.-Y. Lan, W.-Y. Chen, H.-T. Chang, Biosens. Bioelectron. 26 (2011) 2431—2435.
[123] M. Fernandez-Suarez, A. Ting, Nat. Rev. Mol. Cell Biol. 9 (2008) 929—943.
[124] N. Makarava, A. Parfenov, I.V. Baskakov, Biophys. J. 89 (2005) 572—580.
[125] J. Yu, S. Choi, C.I. Richards, Y. Antoku, R.M. Dickson, Photochem. Photobiol. 84 (2008) 1435—1439.
[126] S. Choi, J. Yu, S.A. Patel, Y.-L. Tzeng, R.M. Dickson, Photochem. Photobiol. Sci. 10 (2011) 109—115.
[127] S.-Y. Lin, N.-T. Chen, S.-P. Sum, L.-W. Lo, C.-S. Yang, Chem. Commun. (2008) 4762—4764.
[128] S.-Y. Lin, N.-T. Chen, S.-P. Sun, J.C. Chang, Y.-C. Wang, C.-S. Yang, L.-W. Lo, J. Am. Chem. Soc. 132 (2010) 8309—8315.
[129] Y. Antoku, J.-i. Hotta, H. Mizuno, R.M. Dickson, J. Hofkens, T. Vosch, Photochem. Photobiol. Sci. 9 (2010) 716—721.
[130] X. Jiang, C. Röcker, M. Hafner, S. Brandholt, R.M. Dörlich, G.U. Nienhaus, ACS Nano 4 (2010) 6787—6797.
[131] X. Wu, X. He, K. Wang, C. Xie, B. Zhou, Z. Qing, Nanoscale 2 (2010) 2244—2249.
[132] C. Zhou, M. Long, Y. Qin, X. Sun, J. Zheng, Angew. Chem. Int. Ed. 50 (2011) 3168—3172.
[133] Z. Wu, J. Suhan, R. Jin, J. Mater. Chem. 19 (2009) 622—626.
[134] J.-H. Lee, Y.-w. Jun, S.-I. Yeon, J.-S. Shin, J. Cheon, Angew. Chem. Int. Ed. 45 (2006) 8160—8162.
[135] Y. Jin, X. Gao, Nat. Nanotechnol. 4 (2009) 571—576.
[136] M.A. Habeeb Muhammed, T. Pradeep, Small 7 (2011) 204—208.
[137] X. Le Guevel, B. Hotzer, G. Jung, M. Schneider, J. Mater. Chem. 21 (2011) 2974—2981.
[138] C. Röcker, M. Pötzl, F. Zhang, W.J. Parak, G.U. Nienhaus, Nat. Nanotechnol. 4 (2009) 577—580.
[139] X. Jiang, S. Weise, M. Hafner, C. Röcker, F. Zhang, W.J. Parak, G.U. Nienhaus, J. R. Soc. Interface 7 (2010) S5—S13.

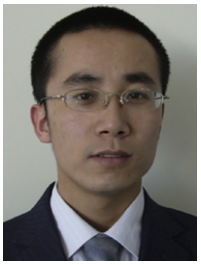

Li Shang graduated with a B.S. degree in chemistry from Wuhan University (P.R. China) in 2004. He obtained his Ph.D. degree in analytical chemistry from Changchun Institute of Applied Chemistry, Chinese Academy of Sciences, under the supervision of Prof. Shaojun Dong in 2009. In 2010 he received a postdoctoral fellowship from the Alexander von Humboldt Foundation and joined the group of Prof. G. Ulrich Nienhaus at the Karlsruhe Institute of Technology (KIT), Germany. He has coauthored over 30 peer-reviewed publications. His scientific interests focus on the development of functional metal nanomaterials for analytical and biomedical applications.

Shaojun Dong, professor of chemistry at Changchun Institute of Applied Chemistry, Chinese Academy of Sciences. She is the member of the Academy of Sciences of the Developing World since 1999. She is currently on the Editorial and Advisory Board of six international journals. She has published over 700 papers in peer-reviewed international journals, the citation by others exceeds 12,000, with an *h*-index of 55. Her research interests concentrate in

electrochemistry with interdisciplinary fields, including chemically modified electrodes, nanomaterials and nanotechnology, bioelectrochemistry, spectroelectrochemistry, and biofuel cells.

Gerd Ulrich Nienhaus is a chair professor and head of the Institute of Applied Physics, Karlsruhe Institute of Technology (KIT), Germany. He obtained his Ph.D. degree in Physical Chemistry from the University of Münster, Germany, in 1988. In 1990, he moved to the Department of Physics of the University of Illinois at Urbana-Champaign, USA, where he was an associate professor before accepting an offer to become chair professor and head of the Institute of Biophysics at the University of Ulm, Germany, in 1996. In 2009, he moved to the KIT. He is a Fellow of the American Physical Society, the Institute of Physics and the American Association for the Advancement of Science. His research focuses on molecular and cellular biophysics studies using a broad array of biophotonics methods.